Ana Rita Santos Oliveira
Bachelors in Biomedical Sciences

Understanding how *Staphylococcus epidermidis* adapts to nitrosative stress generated by the cells of innate immunity

Dissertation to obtain a Master's Degree in Biotechnology

Supervisor: Sandra M. Carvalho, Post-doctoral researcher, ITQB

Co-supervisor: Lígia M. Saraiva, Principal Investigator, ITQB

Jury

President: Ana Cecília Afonso Roque, Phd

Opponent: Susana André Lima Lobo, Phd

Supervisor: Sandra Margarida da Costa Carvalho, Phd

December 2020

FACULDADE DE CIÊNCIAS E TECNOLOGIA
UNIVERSIDADE NOVA DE LISBOA

Bachelors in Biomedical Sciences

Understanding how *Staphylococcus epidermidis* adapts to nitrosative stress generated by the cells of innate immunity

Dissertation to obtain a Master's Degree in Biotechnology

Supervisor: Sandra M. Carvalho, Post-doctoral researcher, ITQB

Co-supervisor: Lígia M. Saraiva, Principal Investigator, ITQB

Jury

President: Ana Cecília Afonso Roque, Phd

Opponent: Susana André Lima Lobo, Phd

Supervisor: Sandra Margarida da Costa Carvalho, Phd

December 2020

FACULDADE DE CIÊNCIAS E TECNOLOGIA
UNIVERSIDADE NOVA DE LISBOA

Understanding how *Staphylococcus epidermidis* adapts to nitrosative stress generated by the cells of innate immunity

Acknowledgments

There are quite a few people without whom the concretization of this process would not be possible and that deserve great words of acknowledgment.

To Dr. Lígia Saraiva, for allowing me to work at the *Molecular Mechanisms of Pathogen Resistance* lab, for supporting every step and turnaround of this work and, or the critical revision of this thesis.

To my supervisor, Sandra, thank you for all the time you spent teaching me, for all your availability and patience for my rookie mistakes, especially during the writing process. You were able to support me in every aspect, even when you could not be present, and keep tabs on my work even from kms away and, for that, I will always be grateful. I could not have asked for someone better to guide me through this journey.

To all my lab colleges, Cláudia, Edit, Jéssica, Joana, Jordi, Laura, Liliana, Marco, Salomé, and Sofia, thank you for always keeping a good mood in the lab, helping me whenever I needed and tolerating the smell of me burning plates.

Às minhas amigas daqui, Juliana e Maria João muito obrigada por todo o apoio e stress partilhados, pelos infinitos áudios de whatsapp que foram sempre capazes de alegrar o pior dia e por me ajudarem a ultrapassar os momentos mais difíceis. Às minha amigas de mais longe, Débora, Raquel, Catarina e Joana, obrigada por não deixarem que a distância signifique esquecimento e por terem arranjado um espacinho nos vossos horários impossíveis, sempre que precisei.

Alberto, obrigada por todo o amor e paciência, por todas as refeições que me cozinhaste, por teres sempre um abraço para mim e por seres o meu porto de abrigo, porque “vai correr tudo bem”.

Aos meus pais, à minha irmã e às minhas avós, obrigada por me terem feito chegar até aqui, por me terem desde sempre incentivado a dar o meu melhor, pelas chamadas eternas a caminho de casa, por me irem buscar à estação de comboio tantas vezes às dez da noite ainda sem jantar para eu não jantar sozinha e por perdoarem todas as minhas ausências.

Resumo

Staphylococcus epidermidis é um microrganismo oportunista que coloniza a pele e mucosas. Esta bactéria é capaz de aderir a dispositivos médicos invasivos, formando biofilmes, que são comunidades de células microbianas rodeadas por uma complexa matriz extracelular e têm um efeito protetor contra antibióticos e o sistema imunitário do hospedeiro. Quando uma infeção ocorre, os macrófagos são recrutados e produzem NO, um composto antimicrobiano. Contudo, vários aspetos da resposta de biofilmes, especialmente de *S. epidermidis,* ao NO continuam inexplorados. Neste trabalho, realizámos uma análise direcionada do perfil metabólico e determinámos a composição do biofilme de *S. epidermidis* para estudar a sua sobrevivência à ação nociva do NO. Observámos que em 1457 e RP62A, duas estirpes clínicas, a quantidade de biofilme foi significativamente diminuída pelo NO, o que não aconteceu em 1457-M12, uma fraca produtora de biofilme. Mostrámos também que, quando exposta ao NO, as quantidades 2 vezes inferiores de biofilme produzidas em 1457, devem-se possivelmente ao seu efeito deletério nas proteínas da matriz e no número de células viáveis, que são respetivamente 2 e 4 vezes menores do que em biofilmes não tratados. Em RP62A, a redução do biofilme na presença de NO pode ser explicada por uma diminuição significativa (4 vezes) na viabilidade celular. Os nossos dados metabólicos indicaram que a resistência das estirpes produtoras de biofilme ao NO foi alcançada através de um aumento na atividade da glicólise e da lactato desidrogenase e da inibição de várias enzimas no nodo do piruvato, ciclo de TCA, metabolismo de amino-açúcar e síntese de PIA. Para melhor elucidar este comportamento, foi iniciada a otimização de um protocolo de extração de metabolitos intracelulares.

Em resumo, este trabalho contribuiu para o avanço do conhecimento sobre a forma como os biofilmes, uma importante causa de infeções resistentes a antibióticos, resistem ao stress nitrosativo.

Palavras-Chave:

Staphylococcus epidermidis, biofilme, stress nitrosativo, metabolismo central de carbono

Abstract

Staphylococcus epidermidis is an opportunistic pathogen that colonizes the human skin and mucosa. When it has the chance, this bacterium adheres to indwelling biodevices where it starts the formation of a biofilm. Biofilms are functional communities of microbial cells surrounded by a complex self-produced extracellular matrix of polymeric substances, which act as a shield against the host immune system and antibiotics. Macrophages, which produce the antimicrobial NO, are among the first cells to be recruited to fight biofilm infections. However, questions such as how biofilms respond to NO and, in particular, how *S. epidermidis* biofilms adapt to NO remain unexplored. In this work, we performed targeted metabolite profiling analysis and biofilm composition determination to uncover how *S. epidermidis* biofilms survive the deleterious action of NO. We observed that NO significantly inhibits biofilm production in two strong biofilm producers, namely 1457 and RP62A strains, but not that in 1457-M12, a weak biofilm producer. Moreover, we showed that the lower biofilm amounts (2-fold) produced in 1457 exposed to NO, are most likely due to the deleterious effect of NO on biofilm matrix proteins and number of viable cells, 2- and 4-fold less than in untreated biofilms, respectively. In RP62A, the lower biofilm amounts in the presence of NO can be explained by a significant decrease (4-fold) in cell viability. Additionally, our metabolic data indicated that resistance of biofilm-producing strains to NO was achieved through an increase in the activity of glycolysis and lactate dehydrogenase, and inhibition of several enzymes at the pyruvate node, TCA cycle, amino-sugar metabolism, and PIA synthesis. To further elucidate this behavior, the optimization of an intracellular metabolite extraction protocol was initiated.

Overall, this work contributed to the advance of knowledge on how biofilms, which are a major cause of antibiotic-resistant infections, resist NO stress of the innate immunity.

Keywords:

Staphylococcus epidermidis, biofilm, nitrosative stress, central carbon metabolism

Table of Contents

Index of figures

Index of tables

List of Abbreviations

Aap	Accumulation-associated protein
Agr	Accessory gene regulator
AK	Acetate kinase
ALS	α-acetolactate synthase
ALSD	α-acetolactate decarboxylase
AMPs	Antimicrobial peptides
APCs	Antigen-presenting cells
AtlE	*S. epidermidis* major autolysin
Bc	Biofilm cells
Bp	Base-pairs
BRc	Biofilm-released cells
CFUs	Colony-forming units
CoNS	Coagulase-Negative *Staphylococci*
CV	Crystal violet
CWA proteins	Cell wall-anchored proteins
DMEM	Dulbecco's Modified Eagle Medium
DNA	Deoxyribonucleic acid
E.	*Escherichia*
e.g.	For example
eDNA	Extracellular DNA
Embp	Extracellular matrix-binding protein
EPS	Extracellular matrix of polymeric substances
Erm^R	Erythromycin resistance
FAD	Flavin adenine dinucleotide
FBS	Fetal Bovine Serum
Fig.	Figure
gDNA	Genomic deoxyribonucleic acid
GMP	Guanosine monophosphate
Hmp	Flavohemoglobin
i.e.	That is
IgG	Immunoglobulin G
iNOS	Inducible nitric oxide synthase
ISC protein	Iron-sulphur cluster protein
LA	Luria-Bertani agar
LB	Luria-Bertani broth
LDH	Lactate dehydrogenase
Mfd protein	Mutation-Frequency-Decline protein
MIC	Minimal inhibitory concentration
MRSA	Methicillin-resistant *S. aureus*
MSCRAMMs	Microbial surface components recognizing adhesive matrix molecules
NAD	Nicotinamide adenine dinucleotide
NADPH	Nicotinamide adenine dinucleotide phosphate

NETs	Neutrophil extracellular traps
NO	Nitric oxide
o/n	Overnight
OD	Optical density
PAMPs	Pathogen-associated molecular pattern
PCR	Polymerase chain reaction
PDH	Pyruvate dehydrogenase
PFL	Pyruvate formate lyase
PGA	Poly-γ-DL-glutamic acid
PIA	Polysaccharide intercellular adhesin
PK	Pyruvate kinase
PNAG	Poly-β(1-6)-N-acetylglucosamine
PPP	Pentose phosphate pathway
PRRs	Pattern-recognition receptors
PSM	Phenol-soluble modulins
PTA	Phosphate acetyltransferase
RIC protein	Repair of iron centres protein
RNS	Reactive nitrogen species
ROS	Reactive oxygen species
RT	Room temperature
S.	*Staphylococcus*
Sar	Staphylococcal accessory regulator
SasG protein	Surface protein G
SesJ	Surface protein J
SigB	RNA polymerase sigma-B factor
SNAP	*S*-nitroso-*N*-acetylpenicillamine
SOE-PCR	Splicing by overlap extension polymerase chain reaction
Spc^R	Spectinomycin resistance
TCA cycle	Tricarboxylic acid cycle
TLR	Toll-like receptors
TSA	Tryptic soy agar
TSB	Tryptic soy broth

1 Introduction

1.1 *Staphylococcus epidermidis*

Staphylococcus epidermidis is a Gram-positive, facultative anaerobe and cluster-forming coccus (Fig. 1.1A) of the *Staphylococcaceae* family[1]. This bacterium is the most common species of Coagulase-Negative Staphylococci (CoNS) found in humans and colonizes asymptomatically every individual's skin (epidermis) and mucosa[1]. An important characteristic of *S. epidermidis* is that it forms biofilms, which are functional communities of microbial cells surrounded by a self-produced extracellular matrix of polymeric substances (EPS)[2,3] (Fig. 1.1B,C).

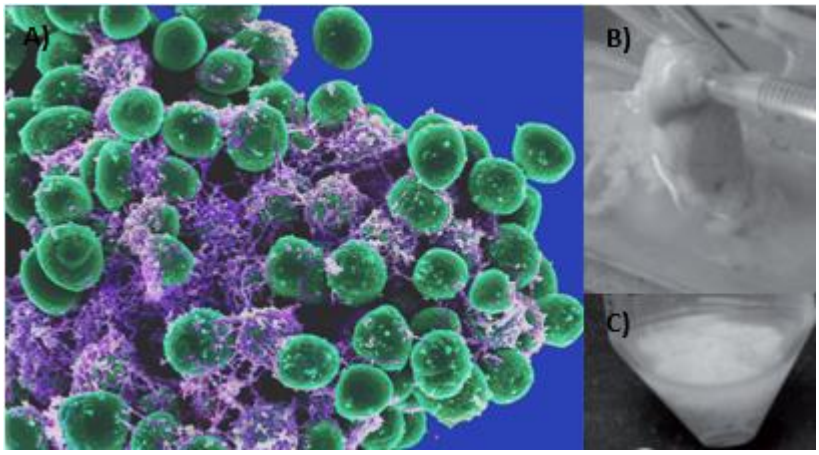

Figure 1.1 - A) Scanning electron microscope image of *Staphylococcus epidermidis* cell clusters embedded in EPS. Adapted from NIAID (https://www.niaid.nih.gov/research/michael-otto-phd), B) and C) Biofilm formed by *Staphylococcus epidermidis* 1457. Adapted from Fey, P and Olson, M 2010.

The ability to form biofilms is what makes *S. epidermidis* a remarkable opportunistic pathogen[4,5]. Indeed, *S. epidermidis* is the major cause of biofilm-associated infections since the increased usage in modern medicine of indwelling medical devices, such as central venous catheters, artificial heart valves, prosthetic joints, ocular lenses, and pacemakers[6,7]. The infections derived from *S. epidermidis* biofilms occur mainly in immunocompromised people and are an important cause of primary bacteremia[8,2]. These infections are often indolent and can be very hard to diagnose, due to the possibility of culture contamination, and to treat[8]. Although in its planktonic form *S. epidermidis* strains may be susceptible to antibiotics, such as linezolid and daptomycin, in biofilms they can present antibiotic resistance[1], which implies an increase in minimal inhibitory concentration (MIC) for the therapeutics. Methicillin resistance, due to the presence of the *mecA* gene[1], has been observed in 70% to 92% of *S. epidermidis* isolates derived from nosocomial infections and is often associated with resistance to other antibiotics[9]. In hospital strains, resistance to aminoglycosides, macrolides, tetracycline, vancomycin, and chloramphenicol has also been found, with variable frequencies[1,10]. Thus, the solution to treat *S. epidermidis* infections is very often the removal of the prosthetics.

S. epidermidis 1457 and RP62A are the two clinical strains used in this work. They were first isolated from infected intravascular catheters[11,12] and, since then, they became used, particularly in biofilm-related research as both were described as strong biofilm producers[12–15]. The 1457 strain has been reported to be compliant with genetic manipulation and susceptible to antibiotics, such as erythromycin[13] and methicillin[16], and RP62A is a methicillin-resistant strain[12,17].

1.1.1 Biofilm as the major virulence factor of *S. epidermidis*

Most of the virulence genes of *S. epidermidis* described in the literature encode proteins and exopolymers involved in biofilm formation (*e.g.* polysaccharide intercellular adhesion PIA) and immune system evasion (*e.g.* poly-γ-DL-glutamic acid PGA, pro-inflammatory molecules), rather than components provoking direct harm to the host[4,5]. For instance, unlike in *S. aureus*, toxins and invasins production in *S. epidermidis* has been rarely observed[1,18]. Even exoenzymes (*e.g.* metaloproteases (SepA), proteases (Esp), and elastases[1,5]) and phenol-soluble modulins (PSM), which can degrade host tissues and membranes, respectively, have a special role in assisting biofilm formation in *S. epidermidis*[2,4,19]. Moreover, the microbial surface components recognizing adhesive matrix molecules (MSCRAMMs) and teichoic acids, which in many pathogens are known to be important for host inflammation processes and colonization, have a major contribution to biofilm formation in *S. epidermidis* through their adhesive properties (*e.g.* to host fibronectin)[1,2,20,21].

Although there is a general lack of knowledge on the mechanisms of pathogenicity of *S. epidermidis*, it is well established that biofilms represent a major virulence factor involved in phenotypic resistance against antibiotics[20].

1.1.2 Biofilm lifecycle

S. epidermidis varies phenotypically between planktonic and sessile life, the latter giving rise to a biofilm community. This switch depends on the growth conditions and is marked by alterations in gene expression[2].

In general, biofilm formation is characterized by different phases of development. The first one is the attachment of planktonic cells to a surface, followed by proliferation of the bacterial cells, maturation of the biofilm, and then detachment[1,2] (Fig. 1.2).

The attachment (Fig. 1.2A) of planktonic cells occurs not only in abiotic surfaces, like prosthetics and catheters, but also in biotic surfaces including the human tissue and the host protein matrix covering the surface of a medical device[1]. The connection between the cells and the surfaces starts with reversible weak interactions[22] (*i.e.* Van der Waals and electrostatic) that are followed by stronger forces, such as hydrogen or ionic bonds[6]. Although dependent on the material used[3], the attachment of cells to abiotic surfaces is usually enabled by hydrophobic interactions and by the action of the *S. epidermidis* major autolysin (AtlE) and accumulation-associated protein (Aap)[2,3]. When the attachment occurs on a biotic surface, MSCRAMMs are the key players[2]. These molecules help the binding of *S. epidermidis* to the host's cells or cell matrix, allowing the bacteria to persist on the surface or inside

the body[1]. *S. epidermidis* has several different MSCRAMMs with specificity to different human matrix proteins like fibrinogen or fibronectin[1].

After the attachment phase, the bacterial cells proliferate, and form aggregates due to adhesive forces (Fig. 1.2B). This phase is characterized by cell division and secretion of biofilm components, creating the EPS[2]. Then, disruptive forces start to occur inside the biofilm, leading to the formation of its characteristic "channels and towers" three-dimensional structure, that allows fluids to travel through the biofilm[2]. This maturation stage is marked by degradation of the biofilm polymers by enzymes, such as nucleases and proteases, and other surfactant-like molecules, namely PSMs, which attack noncovalent interactions. These molecules may also participate in the dispersion or detachment of biofilm cells (Fig. 1.2C) that travel the host organism, eventually starting a second biofilm in a new infection site[2].

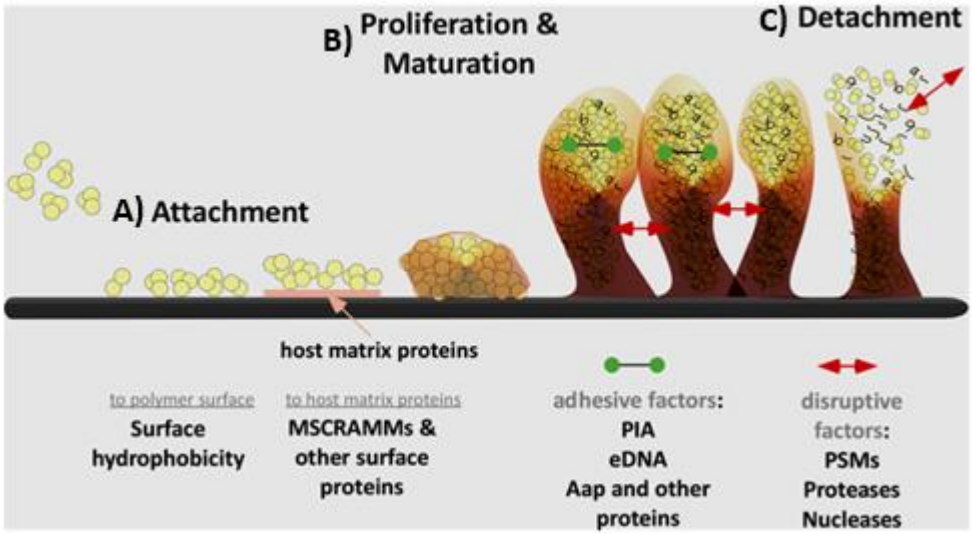

Figure 1.2 - Phases of staphylococcal biofilm formation: attachment, proliferation, maturation, and detachment. Adapted from Otto, M. *et al.,* 2018

All the phases are regulated by several factors, including the Agr quorum-sensing system, a Sar-family regulator, and the alternative sigma factor SigB[2]. The Agr system influences the structure and disruption of the biofilm through the control of PSMs and proteases[2] and is regulated by Sar, which also impacts *ica* (PIA) transcription. SigB is expressed during the stationary growth phase and under stress conditions[2].

1.1.3 Link between central carbon metabolism and EPS production

S. epidermidis is a facultative anaerobe that besides having a respiratory chain, also possesses an Embden-Meyerhof-Parnas (glycolytic), pentose phosphate (PPP) and TCA cycle pathways for the catabolism of glucose (Fig. 1.3). The synthesis of UDP-N-acetylglucosamine, a precursor of PIA, which is a major EPS component in biofilm structures, is linked to glycolysis via the aminosugar pathway (Fig. 1.3)[23–25]. In the transition from a planktonic to a biofilm lifestyle, the cells of *S. epidermidis* shift the metabolism from aerobic respiration to fermentation[2]. Although data regarding the activity of central metabolic pathways in biofilms is not available for *S. epidermidis,* in *S. aureus*

metabolomics and proteomics analysis of biofilms revealed repression of processes like gluconeogenesis, amino acid biosynthesis, oligopeptide uptake and TCA cycle, when compared with planktonic cells[26].

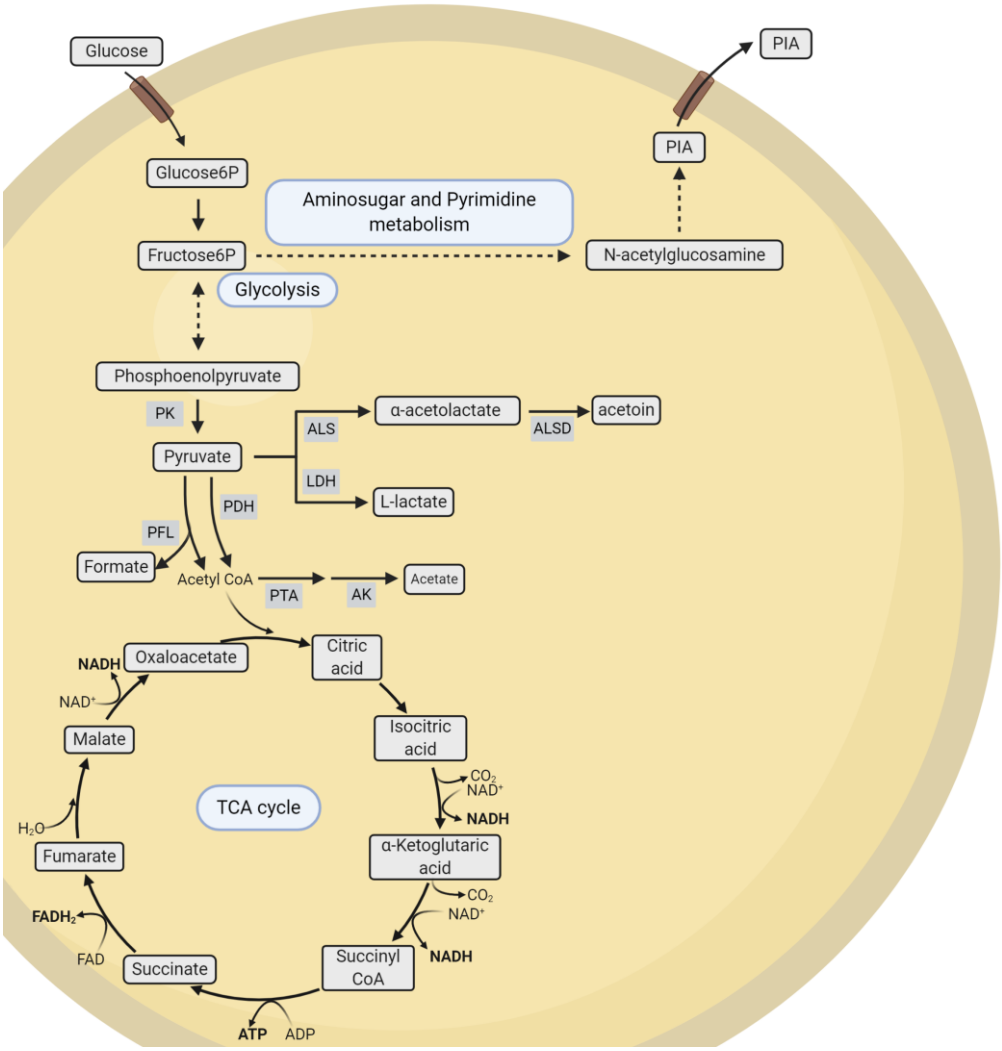

Figure 1.3 – Schematic representation of central carbon metabolic pathways in *S. epidermidis*. Glucose is oxidized to pyruvate via the Embden-Meyerhof-Parnas (glycolytic) pathway. Fructose-6-phosphate, an intermediate of the glycolytic pathway, may be converted to N-acetylglucosamine, a PIA/PNAG precursor, in the amino sugar pathway. Pyruvate can be reduced to several end-products, such as lactate and formate, and/or acetyl-coA, which can be converted to acetate or alternatively to citric acid a TCA cycle intermediate. In exponentially growing biofilms, when comparing with planktonic cells, genes coding for proteins involved in fermentative reactions are upregulated and those coding for proteins of the TCA cycle are downregulated. PK- pyruvate kinase; PDH - pyruvate dehydrogenase; LDH - lactate dehydrogenase; ALS - α-acetolactate synthase; ALSD - α-acetolactate decarboxylase; PFL - pyruvate formate lyase; PTA - phosphate acetyltransferase; AK - acetate kinase. Image created by the author of this thesis, Ana Rita Oliveira in BioRender.

S. epidermidis' EPS is formed mainly by three different types of molecules, namely exopolysaccharides, proteins, that are actively secreted, and extracellular DNA (eDNA), derived from dead cells[2] (Fig. 1.4). Noteworthy, these components are not only part of the biofilm structure but also play an important role in the inhibition of human antimicrobial peptides and phagocytosis[1,2].

One of the main exopolysaccharides of *S. epidermidis* is PIA[1,2], a type of poly-β(1-6)-N-acetylglucosamine (PNAG)[27], which is synthesized from UDP-N-acetylglucosamine by proteins encoded by the *ica* operon (composed by the genes *icaA, icaB, icaC, and icaD*)[1]. The production of PIA is high during the exponential phase of growth when glucose is plenty available and redirected to aminosugar metabolism[28,29] (Fig. 1.4). This redirection of the metabolism has also been associated with a decrease in glycolysis and tricarboxylic acid (TCA) cycle activity[28,29] (Fig. 1.4). Once produced, PIA confers to the biofilm its sticky properties[2], due to its cationic nature, and promotes bacterial cell-cell interactions by binding to the negatively charged elements on the surface of the bacteria[3]. PIA is also a hemagglutinin and can reduce the activity of antimicrobial peptides (AMPs) and neutrophils[1].

The protein content of *S. epidermidis* EPSs may be very diversified[1]. A very important class of proteins in *S. epidermidis* biofilms is the PSMs, that are actively involved in immune evasion, biofilm structuring and although rarely, may also be cytolytic[1,20]. Another relevant protein is Aap which, due to its ability to self-polymerize and form fibrils, is involved in intracellular adhesion[3]. MSCRAMMs, such as the fibrinogen-binding protein SdrG/Fbe[21] and surface protein J (SesJ)[30], are cell wall-anchored (CWA) proteins involved in attachment of the bacterial cells to the host, intracellular interactions, and biofilm formation and maturation[3]. The extracellular matrix-binding protein (Embp) is involved in biofilm formation by being part of the mechanism of adherence to fibronectin[1], a host's protein that plays important roles in cell adhesion[31].

In *S. aureus* the higher production of biofilm proteins was correlated with increased activity of the TCA cycle[32]. Generally, high activity of the TCA cycle was observed for cells exposed to nutrient-limited conditions, such as glucose depletion in the transition from exponential to stationary phase of growth[28,33].

Lastly, eDNA, with its strong anionic character, supports the formation of the biofilm[2] by interacting with other biofilm components, such as proteins and polysaccharides[34]. Moreover, it has been proposed that eDNA has also a role in gene transfer, innate immune response modulation, and nutrient supply[35]. The eDNA originates from cell lysis[2] and although in *S. aureus* TCA cycle inactivation increases the amount of dead cells in the biofilm, it does not influence the amount of eDNA[33]. In *Bacillus subtilis,* increased eDNA production has been correlated with an increase in nucleotide production and a more active TCA[36].

In general, the proportion of the polymeric substances in the extracellular matrix of *S. epidermidis* varies among strains and depends largely on the growth nutritional and environmental conditions and to some extent, on genomic differences, such as the presence of the *icaADBC* genes[37,38].

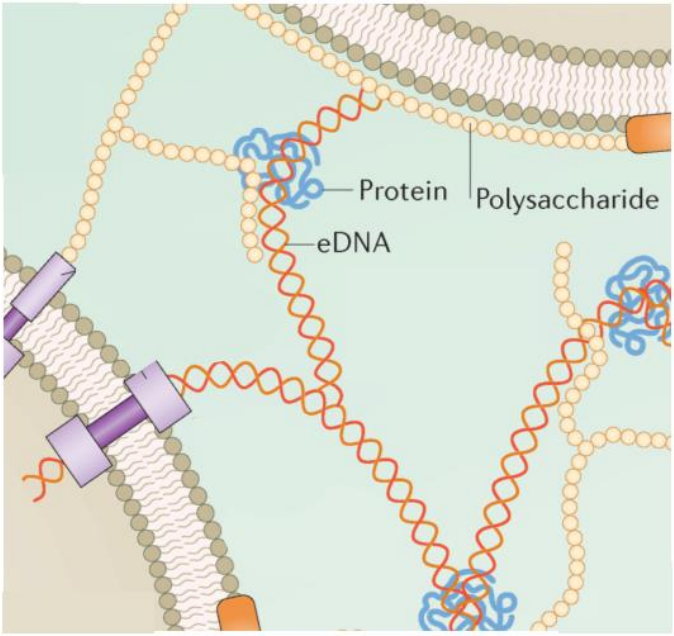

Figure 1.4 – Schematic representation of the EPS showing its main components: exopolysaccharide, protein, and eDNA. Adapted from Koo *et al.*, 2017.

1.2 Immune System response to invasion by biofilm-producing bacteria

Overall, the immune system can be divided into innate and adaptive. Innate immunity, the first to evolve, is very conserved, for example in the animal phyla, and is composed of the complement cascade, toll-like receptors (TLR), and phagocytic cells[39,40]. The innate immune system can distinguish between self and nonself molecules but not among nonself molecules. This inability, if not regulated, leads to an indiscriminate fighting of pathogens and beneficial microorganisms[39]. The adaptive immunity is composed mainly of lymphocytes B and T. These cells can distinguish different nonself molecules or antigens and initiate a response tailored to each pathogen, due to the production of specific receptors (immunoglobulins and T-cell receptors, respectively)[39]. Moreover, they can create a long term memory of the pathogens they encounter during infections and respond faster to further infections[39].

Although being different, innate and adaptive immune systems cooperate, namely through antigen-presenting cells (APCs). The APCs belong to innate immunity and stimulate the adaptive immune cells by presenting them molecules that result from pathogen digestion. On the other hand, the adaptive immune system influences the cells of its counterpart aiming to fight a specific target[39,40].

When biofilm-producing bacteria enter the host organism, they are recognized by pattern-recognition receptors (PRRs), namely TLRs, on the surface of keratinocytes, fibroblasts, and endothelial cells, resulting in the activation of innate immune cells[20] (Fig. 1.5). T-cells, which produce the interferon gamma cytokine responsible for enhancing phagocytes functions, have also been identified in biofilm infections[41]. Generally, *S. epidermidis* is recognized by TLR-2 through bacterial soluble and cell wall components, such as PSM and lipoproteins, respectively[20] (Fig. 1.5). However,

other immune activation routes have also been described. For instance, the biofilm EPS exopolysaccharides, proteins and eDNA were shown to be recognized by TLR-2, TLR-5[42] and TLR-9[43] receptors, respectively. Then, neutrophils and macrophages trigger an inflammatory response involving the coagulation and complement cascades, platelets, extracellular traps (NETs), AMPs, oxygen and nitrogen radicals, and release of cathelicidin and lactoferrin that attack EPS, thus preventing biofilm formation[2,20,41,43,44].

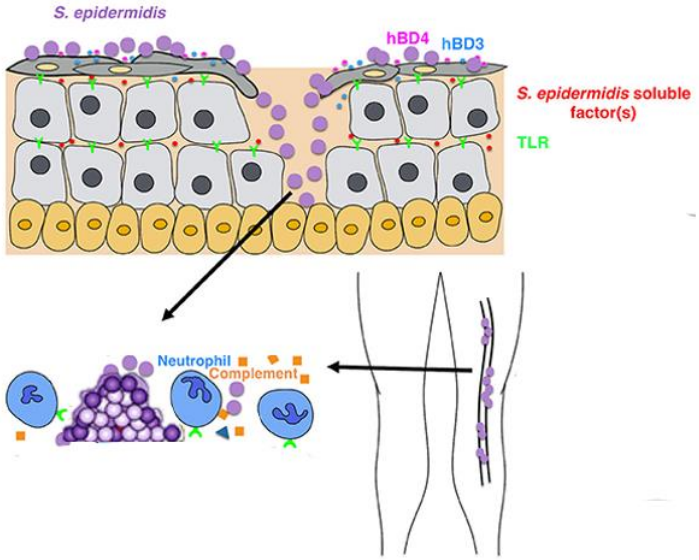

Figure 1.5 – Illustration of the human immune response to *Staphylococcus epidermidis* infection of the skin. After penetration in the intercellular gaps of the skin, *S. epidermidis* (in purple) produces soluble factors (in red) that are recognized by TLR (in green). Neutrophils (in blue) are recruited to the infection sites, AMPs (hBD3 in pink and hBD3 in dark blue) production is induced, and the complement system (in orange) is activated. Adapted from Nguyen, T. *et al.,* 2017 and Reffuveille, F. *et al.,* 2016.

Specifically, inside phagocytes, two main antimicrobial enzyme pathways are activated, the NADPH phagocyte oxidase (Fig. 1.6A) and the inducible nitric oxide synthase (iNOS) (Fig. 1.6B). The activity of these enzymes initiate a cascade of reactions that lead to the formation of reactive oxygen species (ROS) and reactive nitrogen species (RNS), that kill bacteria[45].

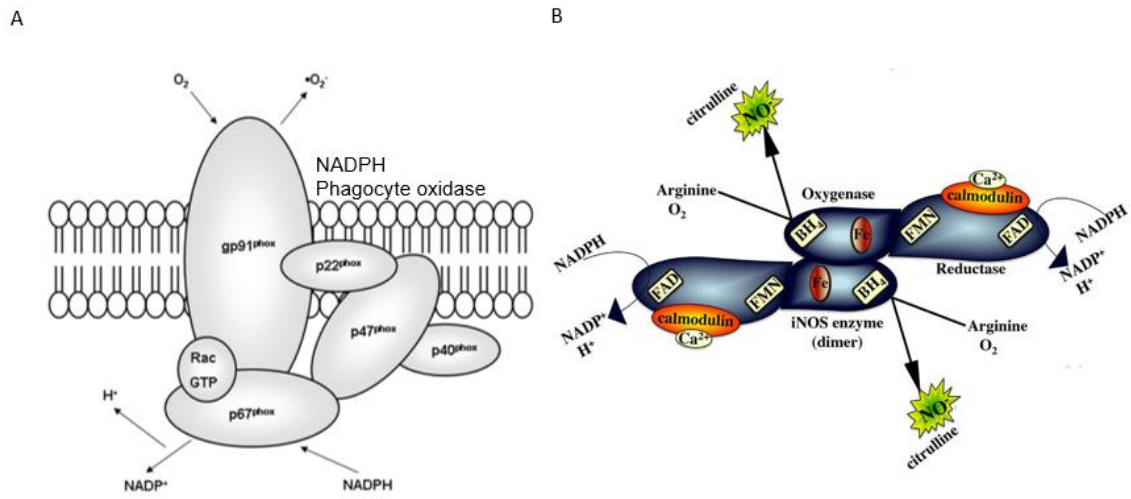

Figure 1.6 – Illustration of enzymatic reactions occurring inside phagocytes when exposed to bacteria (A) Synthesis of superoxide ($O_2^{-\bullet}$) by NADPH phagocyte oxidase, from NADPH and O_2 and (B) Synthesis of nitric oxide ($NO^{\bullet}$) by nitric oxide synthase, from L-arginine, oxygen and NADPH. Adapted from Kellner, M. *et al.,* 2017 and Grayfer, L. *et al.,* 2018.

Nitric oxide synthases catalyze the conversion of L-arginine to L-citrulline and $NO^{\bullet}$, by reducing oxygen and oxidizing NADPH[46] (Fig. 1.6B). There are three different human isoforms of nitric oxide synthases, however it is the inducible isoform 2 or iNOS that produces larger amounts of NO and is involved in the killing of bacteria by phagocytes[45]. In accordance with its name and function, iNOS is not always present in the cells, only being expressed when its transcription is stimulated by molecules, such as proinflammatory cytokines or bacterial lipopolysaccharides[45,46].

NO is known to be involved in several processes, from pathogen control to autoimmune diseases[47], acting as an anti-viral or antimicrobial, pro- or anti-inflammatory, and cytotoxic or cytoprotective substance[47]. Being a diatomic free radical, NO diffuses the bacterial membranes and modifies intracellular targets[48]. Generally, the response of biofilm forming bacteria (*e.g*. *Staphylococcus aureus*, *Bacillus subtilis,* and *Nitrosomonas europaea*) to NO involves changes in their lifestyle[49]. For instance, bacteria exposed to low levels of NO (in the nanomolar range) show an increased transition from biofilm to planktonic lifestyle[50,49] through mechanisms like two-component signal transduction, quorum sensing, and/or cyclic-di-GMP concentration variation[50]. Other studies suggest that high (micromolar) concentrations of NO mutate the DNA of pathogens or prevent DNA repair by altering protein synthesis regulation and modification[47,51,52].

Nitric oxide is converted into other deleterious reactive nitrogen species (RNS), such as nitrogen dioxide ($NO_2^{\bullet}$) and peroxynitrite ($ONOO^-$). These radicals react with different targets inside the cell, namely thiols, metals (*e.g*. in zinc metalloproteins), tyrosines, nucleic acids, and lipids[45,47,53] (Fig. 1.7), thus interfering with cellular processes, such as respiration and DNA replication. Under low oxygen conditions and in the presence of RNS, *S. epidermidis* presents low biofilm formation. In general, cell death and dispersal, induction of *icaR* transcription, and downregulation of the genes coding for Aap and AtlE have been proposed as mechanisms involved in biofilm reduction triggered by NO[51,54,55].

However, in *S. epidermidis,* there is still a big gap in knowledge in what concerns the effect of nitric oxide on the biofilm matrix.

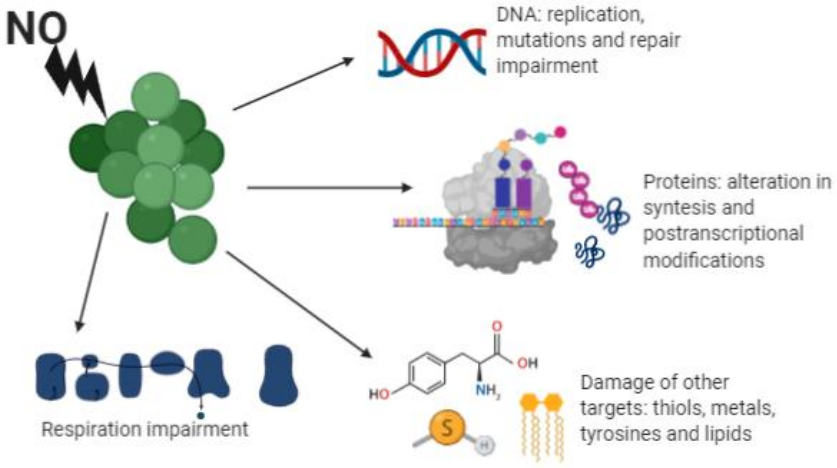

Figure 1.7 – Intracellular targets of nitric oxide in bacteria. Image created by the author of this thesis, Ana Rita Oliveira in BioRender.

1.2.1 Immune system evasion mechanisms of *S. epidermidis* biofilm infections

One of the main strategies of *S. epidermidis* to evade the immune system is through biofilm formation[35]. The high cell density and dense extracellular matrices of the biofilms prevent C3b, a molecule involved in the complement system action, and immunoglobulin G (IgG) deposition, hamper phagocytes movement and bacterial engulfment[2,35,56], and allow horizontal gene transfer and conjugation between bacteria in the biofilm[35]. Moreover, the effect of deleterious molecules, such as AMPs and antibiotics, on the biofilms is less lethal than in floating cells. For instance, the MICs of antibiotics against biofilms are increased 10 to 1000 times relative to those against their planktonic counterparts[2] (Fig. 1.8). Furthermore, biofilms contain “persister” or dormant cells, which due to their low activity in the flow of genetic information and energy metabolism are less responsive to antibiotics[35].

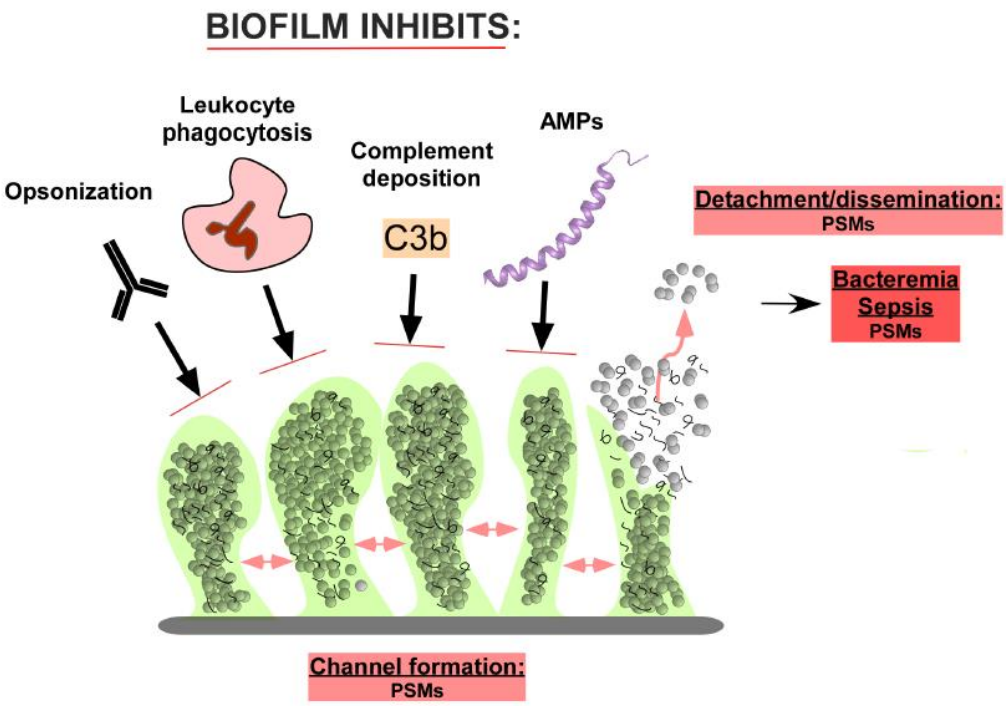

Figure 1.8 – *S. epidermidis* biofilms evading the immune system. The biofilms protect bacteria against opsonization, phagocytosis, complement deposition, and AMPs action. Adapted from Le, K. *et al*., 2018.

1.2.2 Defenses against nitrosative stress of the innate immunity

Most microorganisms have evolved strategies to survive exposure to the antimicrobial nitric oxide (NO), which includes detoxifying enzymes, repair proteins, and metabolic adaptations[50,57–59]. Strategies used by planktonic cells of different bacteria to overcome NO stress are described below.

Detoxifying enzymes

Several NO detoxifying enzymes have been described, among them globulins, flavorubredoxin, and other NO-reducing proteins, being flavohemoglobin the most studied[60]. Flavohemoglobin (Hmp) is a hemoglobin-like protein, which has in its N-terminal a heme-containing globulin and in its C-terminal a NAD and FAD binding domains (oxidoreductase domain). This protein exists in several microorganisms, and is responsible for the detoxification of NO[55,57], by converting nitric oxide into nitrate (NO_3^-) (Fig. 1.9) and nitrous oxide (N_2O), under aerobic and anaerobic conditions, respectively[57]. In *E.coli* and *S. aureus* flavohemoglobin was shown to be active under nitrosative stress conditions, however, its role in *S. epidermidis* is unknown[57].

$$2NO + 2O_2 + NAD(P)H \rightarrow 2NO_3^- + NAD(P) + H^+$$

Figure 1.9 – Chemical equation of NO detoxification by flavohemoglobin, under aerobic conditions.

Repair proteins

DNA and protein damage by nitrogen reactive species prompts the activation of several bacterial systems to repair the altered cell components[61]. Repair of iron centres (RIC) family of proteins[62] and the iron-sulphur cluster (ISC) system[63] are found in several bacteria as nitric oxide is known to attack

the metal centres of proteins[64]. Moreover, DNA damage by nitrosative stress limits bacterial growth in the host, justifying the need for bacterial DNA repair mechanisms. Mutation-Frequency-Decline (Mfd) protein, among other functions, resolves transcriptions halted by DNA damage, and the base excision repair system is responsible for the removal of damaged nucleobases from the DNA backbone[65–67].

Metabolic adaptations

In several microorganisms, nitric oxide is known to attack proteins involved in central carbon metabolism through several different mechanisms. In *S. aureus*, studies showed that NO decreases the activity of the respiratory chain by downregulating *ndhF*, which codes for NADH dehydrogenase subunit 5[68]. Moreover, NO was also shown to inhibit the activity of aconitase (TCA cycle), pyruvate dehydrogenase and pyruvate formate lyase (pyruvate node)[69,70], and to increase the glycolytic activity[58]. Furthermore, nitrosative stress activates important enzymes, namely lactate dehydrogenase (LDH) and alpha-acetolactate synthase (ALS), involved in redox (NAD^+/NADH) and pH balance of the cell[58,59,71–73].

1.3 Aims

Staphylococcus epidermidis is an opportunistic pathogen that was for a long time seen as innocuous[5]. However, in recent years many studies proved that this microorganism is a significant cause of biofilm-associated infections related to the use of indwelling medical devices and called attention to the need of combating this pathogen.

Therefore, it is of main importance to study the mechanisms of biofilm pathogenicity. Regarding the lack of knowledge on how *Staphylococcus epidermidis* biofilms respond to nitrosative stress, an important antimicrobial of the immune system to fight pathogens, in this work we aimed to:

- Construct a *S. epidermidis* mutant of *hmp* (flavohemoglobin), coding a protein known to contribute to NO protection in several microorganisms, and assess the contribution of Hmp to biofilm formation
- Investigate the effect of nitrosative stress on the biofilm formation capacity of *Staphylococcus epidermidis* cells by:
    - determining the amounts of total biofilm and matrix components formed by cells exposed to NO
    - accessing the viability of the biofilm and biofilm released cells under stress conditions
- Study how *S. epidermidis* metabolism adapts and responds to nitrosative stress by:
    - performing metabolite profiling analysis of extra and intracellular metabolites of *S. epidermidis* cells exposed to NO stress
    - analyzing the impact of the metabolic alterations caused by NO on biofilm matrix components

2 Materials and Methods

2.1 Bacterial strains, media, and growth conditions

The strains of bacteria used in this study are listed in Table 2.1 and were stored in 25% (v/v) glycerol (Merck) at -80ºC. Pre-inoculum cultures of *Staphylococcus epidermidis* and *Escherichia coli* were routinely started at 1% (v/v), from -80ºC stocks, in TSB (Difco) and LB (Carl Roth), respectively, and let grown overnight or until exponential phase (4-5 h) at 37ºC and 150 rpm. On Petri dishes, *S. epidermidis* was grown on TSA (Difco) whereas *E. coli* cells were grown on LA (Difco), at 37ºC. When using thermosensitive plasmids, in transformation experiments, *S. epidermidis* and *E. coli* were grown at 30ºC, and when appropriate, liquid and solid media were supplemented with erythromycin (5 µg/mL, Sigma-Aldrich) or with a combination of erythromycin (5 µg/mL, Sigma-Aldrich) and spectinomycin (100 µg/mL, Sigma-Aldrich).

Table 2.1- Strains and plasmids used in this study

Strains/Plasmids	Description	Source
S. epidermidis		
1457	Clinical isolate from a central venous catheter infection, methicillin-sensitive, biofilm (+) and *icaADBC* (PIA) (+)	Rohde, H. University of Hamburg, Germany
1457-M12(also referred in this work as M12)	1457 Δ*purR*::Tn917 mutant, erythromycin resistant, weak biofilm producer and PIA defective, amenable to transformation	Rohde, H. University of Hamburg, Germany
RP62A	Clinical isolate from an intravascular catheter-associated infection, methicillin-resistant, biofilm (+) and *icaADBC* (PIA) (+)	Götz, F. University of Tübingen, Germany
S. aureus		
RN4220	Restriction-defective derivate of NCTC8325-4, Δ*sau1 hsdR*	
E. coli		
DH5α	Transformable *E. coli* K12 derivative	Rohde, H. University of Hamburg, Germany
DC10B	Restriction-defective derivative of *E. coli* K12 DH10B, Δ*dcm*	T. Foster, Trinity College Dublin, Ireland
Plasmids		
pMAD-*hmp*	Thermosensitive pMAD plasmid harboring the *hmp* gene; Spc^R	Laboratory stock
pBASE6	Temperature-sensitive shuttle vector derived from pKOR1 and pBT2	Rohde, H. University of Hamburg, Germany
pBASE6-erm/lox1 or pBASE6-erm/lox2	pBASE6-derived plasmids; Erm^R	Rohde, H. University of Hamburg, Germany

Abbreviations: Spc^R, spectinomycin resistance; Erm^R, erythromycin resistance.
purR, repressor of the *pur* operon (purine synthesis); *dcm,* Dcm methylase (restriction systems)

2.1.1 Growth conditions for biofilm experiments

S. epidermidis cells were grown statically at 37ºC in 4 and 2 mL of DMEM (Gibco, ref. 31966021) supplemented with 10% heat-inactivated fetal bovine serum (FBS, Gibco, ref. 10270106) on 6- and 24- well polystyrene tissue culture plates (Sarstedt), respectively. Alternatively, cells were grown on 96- well plates (Sarstedt) containing 200 µL of TSB. The DMEM+FBS and TSB media were inoculated to an OD_{600} of 0.05 from freshly diluted exponential (4-5h) pre-inoculum cultures of *S. epidermidis* before the filling of the wells (3-4 wells per strain and condition). After 2 hours of incubation at 37ºC, the cells (*circa* 10^8 CFUs/mL) were left untreated or exposed to 1-2 mM (DMEM and TSB media respectively) of freshly prepared DETANONOate (40 mM in 0.01 M NaOH, ACROS Organics) and the plates incubated for more 46 h. The DETANONOate NO donor has a half-life at 37ºC of 20 h.

2.2 Construction of *S. epidermidis* 1457 *hmp* deletion mutants

The oligonucleotide primers used in this work are listed in Table 7.1.

2.2.1 Construction of *S. epidermidis* 1457 *hmp* deletion mutant using pMAD

The construction of the pMAD-*hmp* plasmid (12124 bp) for allelic replacement mutagenesis of the 1457 *hmp* gene and its transformation into *E. coli* DH5α and *S. aureus* RN4220 were not performed in this work and are described in chapter 7.1.1. After transformation of the plasmid into *S. epidermidis* 1457-M12 (chapter 7.2.1) and confirmation of pMAD-*hmp* positive colonies by colony PCR using the primers pairs pMAD_fw and pMAD_rev (chapter 7.2.5), the transformants were grown overnight (o/n) at 30ºC in TSB containing erythromycin and spectinomycin, and two methods for the extraction of the pMAD-*hmp* plasmid from the cells were employed:

1. *QIAprep Spin Miniprep Kit (QIAGEN) combined with peptidoglycan hydrolytic enzymes and bead beating.* 4 mL of the o/n culture were centrifuged at 6800 *x g* for 3 min. The resulting cell pellet was resuspended in 250 µL of buffer P1 (QIAGEN) and digested with lysostaphin (0.08 mg/mL, Sigma-Aldrich), lysozyme (4 mg/mL, Sigma-Aldrich) and mutanolysin (0.08 KU/mL, Sigma-Aldrich), at 37ºC for 1 h. Cells were then disrupted by bead beating (Minilys personal homogenizer, BERTIN INSTRUMENTS) with two 1-min cycles at 5000 rpm, with 1-min intervals on ice. After bead removal (centrifugation at 11337 x *g* for 10 min), 250 µL of buffer P2 (QIAGEN) was added to the supernatant and the protocol was finished according to the QIAprep Spin Miniprep Kit manufacturer's guidelines.

2. *Alkaline lysis plasmid extraction method*. The alkaline lysis extraction method was performed as in Lindgren, J. 2014[74] and is described as follows., 8 mL of the o/n culture were centrifuged for 10 min, at 6000 x *g*. Then, cell pellets were homogenized in 1 mL of 3% (w/v) sodium chloride (Carl Roth), centrifuged again at 6000 *x g* for 10 min and resuspended in 150 µL of a

solution containing 20 mM Tris–HCl (Carl Roth, CARLO ERBA), 50 mM EDTA (Carl Roth) and 0.58 M sucrose (Sigma-Aldrich), pH 7.5. Afterward, lysostaphin (0.07 mg/mL, Sigma-Aldrich) and lysozyme (13 mg/mL, Sigma-Aldrich) were added, and the homogenized cells were placed on a 37ºC water bath for 30 min to allow high activity of the enzymes. Once the enzymatic digestion was completed, the samples were suspended in 300 µL of fresh 0.1 M NaOH (EKA) and 1% SDS (Carl Roth) solution and incubated on ice for 5 min. Then, 225 µL of potassium acetate (1.5 M, pH 4.8, Merck) was added to the digested samples and these were again incubated on ice. The cell lysate was centrifuged at 10000 *x g* for 10 min and the supernatant was transferred to a new microcentrifuge tube containing 500 µL of a phenol:chloroform:isoamyl alcohol (25:24:1, Carl Roth, Merck, Sigma-Aldrich) solution, to allow for separation of proteins. The tubes were vortexed and centrifuged at 11337 *x g* for 5 min and the top aqueous layer that contains nucleic acids was transferred to a new microcentrifuge tube, where two volumes of 100% ethanol were added to precipitate the DNA. The tubes were then frozen at -80ºC for 20 min. Subsequently, the samples were centrifuged for 15 min at 12000 *x g* and 1 mL of 70% ethanol (Merck) was added to the pellet. After centrifugation in the same conditions, the tubes were left open in the hotte for about 1 h until all the ethanol has evaporated. The DNA pellet was dissolved in 40 µL of milli-Q water.

The extracted DNA was quantified in a Nanodrop ND-1000 UV-visible spectrophotometer (Thermo Fisher Scientific) and visualized on a 1% agarose gel in TAE buffer after a run at 80V, 400 mA for 40 min.

2.2.2 Construction of *S. epidermidis* 1457 *hmp* deletion mutant using pBASE6 and pBASE6-derived plasmids

pBASE6

In 1457 strain, the *hmp* gene forms a monocistronic operon. For the construction of the pBASE6-*hmp* plasmid (8554 bp), the upstream (1156 bp, fragment A) and downstream (867 bp, fragment B) regions of the *hmp* gene were PCR amplified from the 1457 genomic DNA using the following pairs of primers: *hmp*_fw_A / *hmp*_rev_A and *hmp*_fw_B / *hmp*_rev_B (Table 7.1 and 7.2). The resulting PCR products and pBASE6 plasmid, which was extracted from *E. coli* DH5α using the QIAprep® Spin Miniprep Kit (QIAGEN), were digested with EcoRI, XmaI and EcoRV. Afterward these fragments and the linearized pBASE6 were ligated (Table 7.3) using T4 DNA ligase (NEB), at 16ºC for 16 hours in two different ways. First, by performing a single reaction with both fragments and the plasmid and secondly, by ligating fragments A and B and then the resulting AB fragment to the plasmid (Fig. 2.1). This construction was then transformed by chemical competence into *E. coli* DC10B, which was grown at 30ºC (chapter 7.2.4). The screening for positive colonies was performed by colony PCR (chapter 7.2.5).

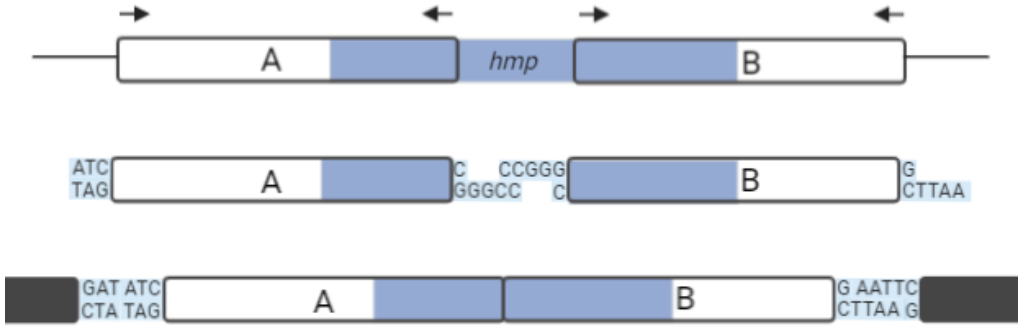

Figure 2.1 – Schematic representation of the construction of the pBASE6_*hmp* plasmid. Fragments A and B represent the upstream and downstream regions of the *hmp* gene (in blue) from *S. epidermidis* 1457 genome. The arrows indicate primers used to amplify the A and B fragments. Enzymatic digestion of the fragments A and B and of pBASE6 plasmid exposes blunt and cohesive ends that allow ligation of both fragments and to the digested pBASE6 plasmid, creating the pBASE6_*hmp* plasmid.

pBASE6-erm/lox1 and pBASE6-erm/lox2

The pBASE6-erm/lox plasmids 1 and 2 (9855 bp) are derived from pBASE6 plasmid and contain erythromycin cassettes (chapter 7.1.2), allowing for selection of erythromycin resistant clones. For the construction of pBASE6-erm/lox1_*hmp* and pBASE6-erm/lox2_*hmp* plasmids, up- (1167 bp, A) and downstream (878 bp, B) DNA fragments of *hmp* were obtained by PCR amplification using the primer pairs 2*hmp*_fw_A / 2*hmp*_rev_A and 2*hmp*_fw_B / 2*hmp*_rev_B (Table 7.1) and gDNA of 1457 as template. Then, the resulting fragments A and B were digested with SalI/NheI and SacI/EcoRI, respectively, and cloned one at a time into the SalI/NheI and SacI/EcoRI sites of pBASE6-erm/lox plasmids (Fig. 2.2). *E. coli* DC10B (chapter 7.2.4) was used as the cloning host. Transformants were selected in LA with erythromycin and screened for plasmid incorporation by colony PCR (chapter 7.2.5). Alternatively, fragments A and B amplified with the primer pairs 2*hmp*_fw_A / A_Erm and B_Erm / 2*hmp*_rev_B, respectively, were by means of splicing by overlap extension polymerase chain reaction (SOE-PCR) fused to an Erm^R gene amplified from pBASE6-erm/lox2 with the primers Erm_fw and Erm_rev (Table 7.1). The resulting fragment (Fig. 2.3) was visualized on a 1% agarose gel in TAE buffer (ran at 80V, 400 mA for 40 min), extracted and purified using the QIAquick® Gel Extraction Kit (QIAGEN).

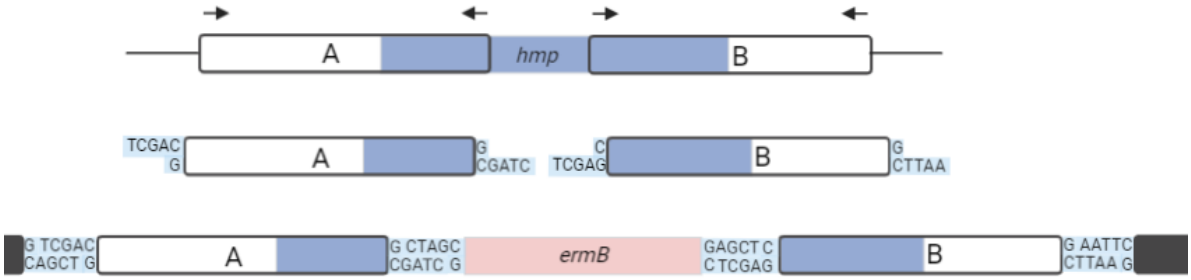

Figure 2.2 – Schematic representation of the construction of the pBASE6-erm/lox1_*hmp* and pBASE6-erm/lox2_*hmp* plasmid. Fragments A and B represent the upstream and downstream regions of the *hmp* gene (in blue) from *S. epidermidis* 1457 genome. The arrows indicate primers used to amplify the A and B fragments. Enzymatic digestion of the fragments A and B and of pBASE6-erm/lox1 and pBASE6-erm/lox2 exposes cohesive ends that allow for ligation of the fragments, one at a time, around the ermB cassette (in pink), in the digested pBASE6-erm/lox1 and pBASE6-erm/lox2 plasmids, creating the pBASE6-erm/lox1_*hmp* and pBASE6-erm/lox2_*hmp* plasmids.

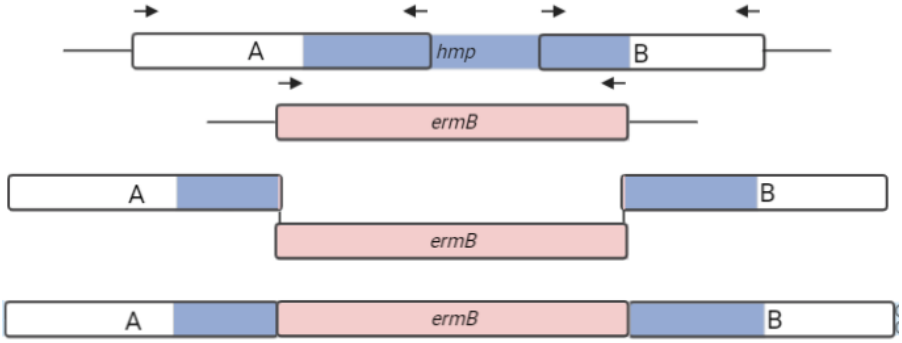

Figure 2.3 – Schematic representation of the construction of the AermBB fragment using SOE-PCR. Fragments A and B represent the upstream and downstream regions of the *hmp* gene (in blue) from *S. epidermidis* 1457 genome and ermB represents the erythromycin resistance cassette (in pink) in the pBASE6-erm/lox2 plasmid. The arrows indicate primers used to amplify the A, B and ermB fragments. A and B fragments include a sequence complementary to the ermB fragment (in pink) which allows for a SOE-PCR reaction to ligate the three fragments, forming the AermBB fragment.

2.3 Assays for the quantification of biofilm components

S. epidermidis biofilms of 1457-M12, 1457, and RP62A strains, exposed and unexposed to NO, were grown on 24- and 96- wells flat plates in DMEM+FBS and TSB, respectively, as described above. For the determination of the relative amount of protein, the 48 h biofilms were treated with sodium periodate (40 mM, Sigma-Aldrich) for 24 h at 4ºC. On the other hand, biofilm exopolysaccharide levels were determined by treatment with proteinase K (1mg/mL, Sigma-Aldrich) for 4 h at 37ºC. Subsequently, biofilms were washed 1 to 2 times with PBS (1x – 10 mM Na_2HPO_4 (Carl-Roth), 1.8 mM KH_2PO_4 (Sigma-Aldrich), 137 mM NaCl (Carl Roth), 2.7 mM KCl (Carl Roth), pH 7.4) and heat-fixed at 65ºC for at least 2 h. Biofilms were then stained with crystal violet (CV) as follows: 2 mL (for 24-wells plates) or 200 µL (for 96-wells plates) of CV (1% (v/v), Merck) were added to each well and stained biofilms incubated for 20 min at RT. Afterward, each well was washed twice with 1 volume of PBS (1x) and 1 volume of glacial acetic acid (33% (v/v), Carlo Erba) was added. After

10 min of incubation, the crystal violet resuspended in the glacial acetic acid, and CV absorption was read at 590 nm. Untreated biofilms were also stained with CV to obtain the total amount of biofilm.

2.4 Biofilm and biofilm released cell viability

Cell viability in the biofilms and in the supernatant was determined. The medium in each well was collected to a microcentrifuge tube. The biofilms were collected from the 24- and 96- well plates to microcentrifuge tubes in 1 mL or 100 µL of PBS (1x), respectively. Then, the buffered biofilms were vortexed for 30 sec, sonicated (Bioruptor® Plus Sonication System) for 12 cycles (10 sec ON, 30 sec OFF, on high setting), vortexed again and centrifuged at 11337 *x g* for 1 min at RT. The resulting cell pellets were suspended in 2 mL or 200 µL of PBS (1x). For both cases, serial dilutions were plated, and colony-forming units formed per mL were counted.

2.5 Preparation of samples for quantification of extracellular metabolites by ^{1}H-NMR

S. epidermidis biofilms were grown as described above for 48 h and 100 µL of the floating media were collected and centrifuged at 1000 *x g* for 1 min. After that, 200 µL of cold (-80ºC) LC-grade methanol (Merck) were added to each supernatant, the mixtures were incubated in dry ice for 30 min and then centrifuged at 16000 *x g*, at 4ºC for 20 min for the precipitation of FBS. The supernatants were placed in a N_2 streaming for approximately 2 h until all the methanol had evaporated and the precipitates were stored at -20ºC until further analysis. The metabolites present in the samples were analyzed by ^{1}H-NMR, as described before[58].

2.6 Optimization of intracellular metabolite extraction protocols from *S. epidermidis* 1457 biofilms

S. epidermidis 1457 biofilms, untreated or treated with NO, were grown in 6-well plates in DMEM+FBS, as described above. Extraction of intracellular metabolites was performed by four different techniques, based on previous protocols[75–77], as follows.

1. Biofilms were resuspended in 10 mL of a saline solution (0.85% (w/v), Carl Roth) at 30ºC, filtered (0.22 micron filter, Millipore), washed twice with the same saline solution, and frozen in liquid nitrogen. To extract the metabolites, 1 mL of methanol at -20ºC (Merck), 1 mL of chloroform at -20ºC (Merck) and 0.9 mL of ice-cold Milli-Q water were sequentially added to the biofilms. After each addition, the cells were immediately vortexed for 1 min. The mixture was centrifuged at 7215 *x g* at –10ºC for 10 min.

2. The biofilms were resuspended in 6 mL of ice-cold PBS (1x) and centrifuged at 3200 *x g* for 10 min at 4 °C. Then 1.6 mL of ice-cold aqueous methanol (Merck) at 80% (v/v) were added to the pellets and the solutions were incubated at -80ºC for 1 h. After incubation, addition of 2.4 mL chloroform (Merck) to the cells was performed and the mixtures vortexed five times for 30 sec with 1-

min intervals on ice. Subsequentially, the cells were mixed with 2 mL of 0.2 M ammonium hydroxide (Honeywell Fluka), vortexed as before and then centrifuged at 3200 *x g* for 15 min at 4 °C.

3. Biofilms were resuspended in 6 mL of sterile PBS (1x) and centrifuged at 1482 *x g* and 25ºC for 10 min. The pellets were immediately frozen in liquid nitrogen, washed with 24 mL of 60% ice-cold methanol (Merck), centrifuged at 1677 *x g* at 25ºC for 10 min and resuspended in 1 mL of a 2:1 ice-cold methanol/chloroform solution (Merck). The cells were then sonicated for 15 min in a bath sonicator (Branson 5200 Ultrasonic Cleaner) and afterward 1 mL of 1:1 aqueous chloroform solution (Merck) was added to the cells. The samples were centrifuged at 1677 *x g* and 25ºC for 10 min.

4. Biofilms were collected in 6 mL of ice-cold PBS (1x) and centrifuged at 3200 *x g* and 4ºC for 10 min. The pellets were resuspended in 1 mL of 2:1 ice-cold methanol/chloroform solution (Merck), sonicated 3 x 10 sec (30% power, ~50 pulse, Dr Hielscher UP200S) and then 300 µL of a 1:1 aqueous chloroform (Merck) solution were added to the cells. The mixtures were vortexed 3 x 10 sec and centrifuged at 3200 *x g* and 4ºC for 10 min.

All the final supernatants were lyophilized and stored at -80ºC until analysis by ^{31}P-NMR, as previously described[78].

2.7 Statistical analysis

The program used for statistical analysis was GraphPad Prism (GraphPad software version 5.01, California, USA). Comparison of the results was made using two-tailed unpaired t-tests with a 95% confidence interval.

2.8 Author contributions

Ana Rita Oliveira performed all the work of this thesis, with the exception of the construction of pMAD-*hmp* plasmid and NMR analyses. The pMAD-*hmp* plasmid was constructed by Cláudia Freitas and NMR analyses were done by Drª Sandra Carvalho.

3 Results and Discussion

In hosts, *Staphylococcus epidermidis* biofilms are exposed to nitric oxide and other deleterious reactive nitrogen species generated from cells of the innate immunity[51,79,80]. In general, bacterial pathogens defend against NO by activating detoxifying enzymes and repairing proteins and by means of complex metabolic adaptations[50,55]. Despite the clinical relevance of *S. epidermidis*, due to biofilm infections, proteins and metabolic adaptation mechanisms involved in the survival of this bacterium to NO remain largely unknown. In this work, we proposed to elucidate: 1) the physiological function of Hmp in *S. epidermidis* biofilms exposed to NO by deleting the *hmp* gene of strain 1457; 2) the role of central carbon metabolism in the adaptation of *S. epidermidis* 1457 to NO and its implications in biofilm formation.

3.1 Construction of a *hmp* mutant of *S. epidermidis* strain 1457

The *S. epidermidis* 1457 genome contains a gene predicted to encode a flavohemoprotein like protein (*hmp*, B4U56_10385). Thus, this gene was selected for allelic replacement mutagenesis to determine its function.

3.1.1 Construction of *S. epidermidis* 1457 *hmp* mutant using the pMAD plasmid

Stocks of the pMAD-*hmp* plasmid (12124 bp) were already available in our laboratory. The construction of this plasmid and its transformation into *E. coli* DH5α and *S. aureus* RN4220 is described in chapter 7.1.1 and was based on literature protocols[81]. In this work, the pMAD-*hmp* plasmid was transformed into *S. epidermidis* 1457-M12, and Spc^R positive transformants were identified by colony PCR (Fig. 3.1). It should be noted that the choice to transform 1457-M12 prior to 1457 was based on the description that electroporation to deliver plasmids into other *S. epidermidis* strains, such as 1457, is more efficient after their passage in PIA- and biofilm-defective mutant 1457-M12[82,83]. The positive colonies showed bands in the agarose gel between 2000 and 3000 bp, which match the expected size of the colony PCR product (2727 bp) that confirms the presence of the pMAD-*hmp* plasmid (Fig. 3.1).

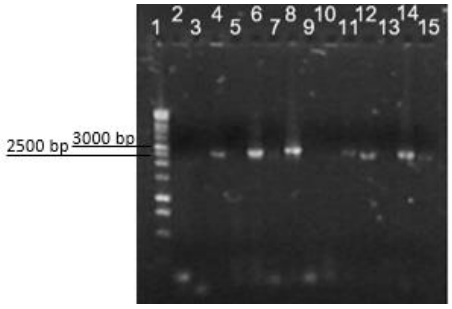

Figure 3.1 – Agarose gel showing the products amplified by 1457-M12 colony PCR using the primers pMAD_fw and pMAD_rev (Table 7.1) to confirm the presence of the pMAD-*hmp* plasmid. Colony PCR products from 14 colonies (lanes 2 to 15) are shown, from which 7 showed the expected band size of 2727 bp. The electrophoresis was performed in 1% agarose gel in TAE buffer, 80V, 400 mA for 40 minutes using a 1 kb ladder (lane 1).

To extract the pMAD-*hmp* plasmid from the *S. epidermidis* 1457-M12 strain we have employed several extraction methods designed for staphylococci, but only two resulted in significant extraction of DNA (chapter 2.2.1 and Fig. 3.2).

Optimization of DNA plasmid extraction with a commercial kit

In *S. epidermidis* 1457-M12 strain, the extraction of the pMAD-*hmp* plasmid using the QIAprep Spin Miniprep Kit (QIAGEN) technique, which involves chemical lysis, combined with lysozyme and lysostaphin digestion, did not result in significant amounts of DNA (data not shown). In our laboratory, this method has been successfully used to extract plasmid DNA from *Staphylococcus aureus* RN4220 (up to 2.6 µg). Lysozyme is a MurNAcβ(1→4)GlcNAc peptidoglycan hydrolase and lysostaphin is a glycylglycine endopeptidase that cleaves the cross-linking pentaglycine bridges of the peptidoglycan of several staphylococci species[84,85]. Even though the resistance of staphylococci to traditional methods of lysis, such as lysozyme and detergents[74,86], is common and the resistance of *S. epidermidis* to lysostaphin is dependent on the amount of glycine residues that are replaced by serine in the pentapeptide cross-bridges[85,87], an unsuccessful extraction of the plasmid from 1457-M12 strain was not expected. Thus, we hypothesized two scenarios: cell lysis in *S. epidermidis* was hampered by the presence of matrix polymers surrounding the cell wall, namely polysaccharides and poly-γ-DL-glutamic acid (PGA), which are far more abundant in *S. epidermidis* than in *S. aureus*[22,88,89], and/or *S. epidermidis* possesses a resistance mechanism that shielded, inhibited or destroyed the activity of the peptidoglycan hydrolytic enzymes. In accordance with these hypotheses, the addition of a step that consisted of mechanical disruption with beads, used in several DNA extraction methods[90–92], and mutanolysin, an enzyme that targets the peptidoglycan MurNAcβ(1→4)GlcNAc linkages in O-acetylated peptidoglycans, widely used to lyse *Streptococcus pneumoniae* cells[93,94], increased the yield to 2.6 µg of DNA. It should be noted that the amounts of DNA extracted by adding bead beating and mutanolysin separately to the initial protocol, involving the use of the Qiagen kit with added lysozyme and lysostaphin digestion, were significantly lower (at least 6.5-fold) than those obtained by adding both bead beating and mutanolysin.

Plasmid DNA extraction by alkaline lysis

The alkaline lysis method for the extraction of DNA in *S. epidermidis* strains[87], which involves chemical lysis[95], was used to isolate the pMAD-*hmp* plasmid from *S. epidermidis* 1457-M12, yielding 8 µg of DNA, a value 3-fold higher than that obtained with the QIAprep Spin Miniprep Kit (QIAGEN) combined with lysozyme, lysostaphin, mutanolysin, and bead beating.

Although we obtained significant amounts of DNA to proceed with *S. epidermidis* 1457 transformation, the extracted DNA from 1457-M12 did not correspond to the pMAD-*hmp* plasmid (12124 bp), as shown by the band profile, on agarose gel, when comparing with that of pMAD-*hmp* previously extracted from *S. aureus* RN4220 (Fig. 3.2). Further confirmation was performed by digesting the DNA with EcoRV, which did not originate the expected two bands of 4233 bp and 7891 bp, as obtained from the digestion of pMAD-*hmp* extracted from RN4220 (Fig. 3.3). Most likely, the isolated DNA corresponds to the cryptic plasmid (> 10 kb) of *S. epidermidis* 1457[96].

An answer to the question as to why we lost the pMAD-*hmp* plasmid present in 1457-M12 colonies is difficult to put forward. A possible explanation is the loss of the pMAD-*hmp* plasmid during the 36 h growth of 1457-M12 at 30ºC in TSB containing erythromycin and spectinomycin before extraction. Competition of the cryptic plasmid with pMAD-*hmp* by two different strategies was also hypothesized. As it has been described, two different but related plasmids cannot coexist stably in the same host cell, especially when competing for replicatory machinery[97]. However this is not very likely, as pMAD is derived from pE194[81], a plasmid that names one of the four main groups of small (<8 kb) staphylococci plasmids, defined by their replication initiation gene, and the extracted plasmid is bigger than 10 kb and hence probably in a different incompatibility group[98]. It may also happen due to partitioning incompatibility[99,100], since there is no information about the segregation strategy of the extracted plasmid. Considering the difficulty of plasmid curation from *S. epidermidis* strains, we proceeded with a new approach to construct the *hmp* mutant.

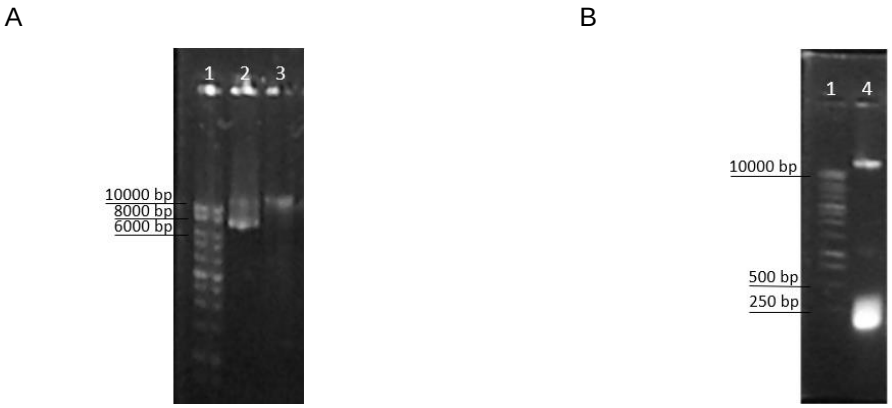

Figure 3.2 – Plasmid DNA extracted from *S. aureus* RN4220 (A, lane 2) and *S. epidermidis* 1457-M12 (A, lane 3 and B, lane 4) using the QIAprep Spin Miniprep Kit from QIAGEN combined with hydrolytic enzymes and bead beating (A) and the alkaline lysis method (B). The electrophoresis was performed in 1% agarose gel in TAE buffer at 80V, 400 mA for 40 minutes. 1 Kb ladder (lane 1) was used as marker.

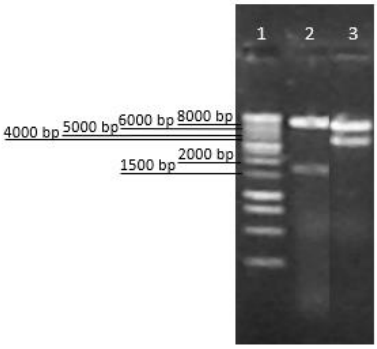

Figure 3.3 – DNA fragments that resulted from EcoRV digestion of the extracted plasmid DNA. Lane 2, digested DNA plasmid extracted from *S. epidermidis* 1457-M12; lane 3, digested pMAD-*hmp* from *S. aureus* RN4220. Expected size of the fragments: 4233 and 7891 bp. The electrophoresis was performed in 1% agarose gel in TAE buffer at 80V, 400 mA for 40 minutes. 1 Kb ladder (lane 1) was used as marker.

3.2 Construction of *S. epidermidis hmp* mutant using pBASE6 and pBASE6-derived plasmids

The use of pBASE6, a markerless plasmid, and pBASE6-erm/lox1[101] and pBASE6-erm/lox2[102], which contain a selection marker (*ermB* gene), to construct *S. epidermidis* mutants by allelic replacement mutagenesis has been performed before[101–103], and is also described in chapter 7.1.2. In this work, recombinant plasmids, namely pBASE6-*hmp*, pBASE6-erm/lox1-*hmp,* and pBASE6-erm/lox2-*hmp* were constructed by cloning the flanking regions of *hmp* into pBASE6 and pBASE6-erm/lox1 and 2 or by fusing the flanking regions of *hmp* with an ermB fragment (SOE-PCR) and then cloning into pBASE6-erm/lox2 (please see chapter 2 for details). Briefly, the upstream (A fragment) and downstream (B fragment) regions of the *hmp* gene were PCR-amplified from 1457 gDNA (Fig. 3.4A-C) and the *ermB* gene was amplified from pBASE6-erm/lox2 (Fig. 3.4D). The pBASE6, pBASE6-erm/lox1[101] and pBASE6-erm/lox2[102] plasmids were extracted from *E. coli* DH5α (Table 2.1, Fig. 3.4E-F).

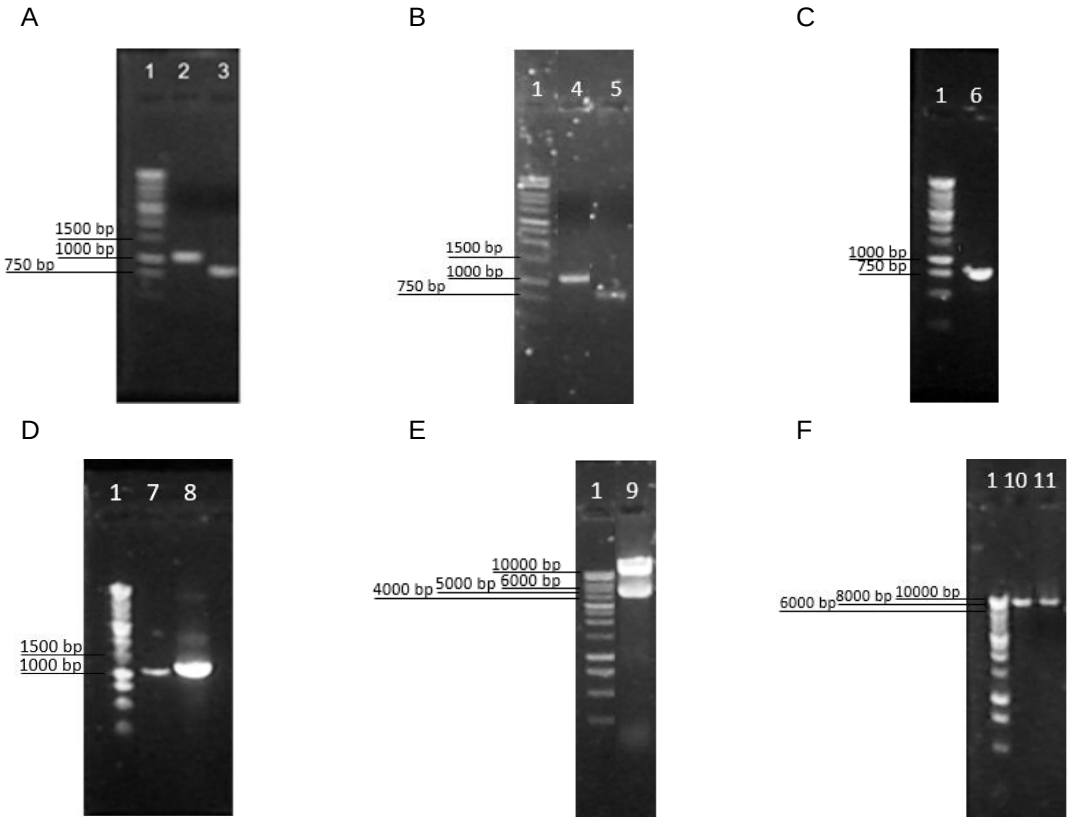

Figure 3.4 – Upstream and downstream fragments of *hmp* and extracted pBASE6 plasmids. (A) fragments A (2, 1156 bp) and B (3, 867 bp) for the construction of pBASE6-*hmp*. (B) fragment A (4, 1156 bp) and B (5, 867 bp) for the construction of pBASE6-erm/lox1-*hmp* and pBASE6-erm/lox2-*hmp*. (C and D) fragment B (6, 878 bp), A (7, 1167 bp), and ermB (8, 1301) for the construction of pBASE6-erm/lox2-*hmp* via SOE-PCR. (E) pBASE6 plasmid (9, 6600 bp). (F) pBASE6-erm/lox1 (10, 7880 bp) and pBASE6-erm/lox2 (11, 7880 bp). The electrophoresis was performed in 1% agarose gel in TAE buffer at 80V, 400 mA for 40 minutes and ran with a 1 kb ladder (lane 1).

The fragments and the plasmids were then digested (Fig. 3.5), ligated to create pBASE6-*hmp*, pBASE6-erm/lox1-*hmp* or pBASE6-erm/lox2-*hmp* and transformed into *E. coli* DC10B, as described before[101,102]. The passage of plasmid DNA through *E. coli* DC10B prior to electroporation into *S. aureus* and *S. epidermidis* has been shown to bypass the *S. epidermidis* type IV restriction system due to the absence, in DC10B, of a functional Dcm methylase, which is responsible for methylating the second cytosine of the CCTGG and CCAGG sequences[104]. To check for pBASE6-*hmp*, pBASE6-erm/lox1-*hmp* and pBASE6-erm/lox2-*hmp* positive clones, 42, 15 and 12 isolated colonies were selected, respectively, and colony PCR with pBASE6 hybridizing primers was performed. However, none of the colonies were found to contain the expected band sizes (Fig. 3.6 and 3.7). Moreover, no bands were observed by PCR of DC10B colonies transformed with the empty plasmid (data not shown). These results suggest that transformation was not efficient and/or the triple ligation of A and B fragments to the plasmid, simultaneously or one at a time, did not occur.

Although it is commonly used, the cloning method based on restriction and ligation becomes more difficult as the number of fragments increases[105]. Moreover, the efficiency of the ligation step can be influenced by DNA concentration and purity[106,107]. Even though all the used DNA was analyzed by gel electrophoresis, the presence of nucleic acid contaminants with similar sizes than the expected fragments cannot be excluded and can result in the disturbance of subsequent enzyme-catalyzed reactions by blocking access to restriction sites or overhangs[106].

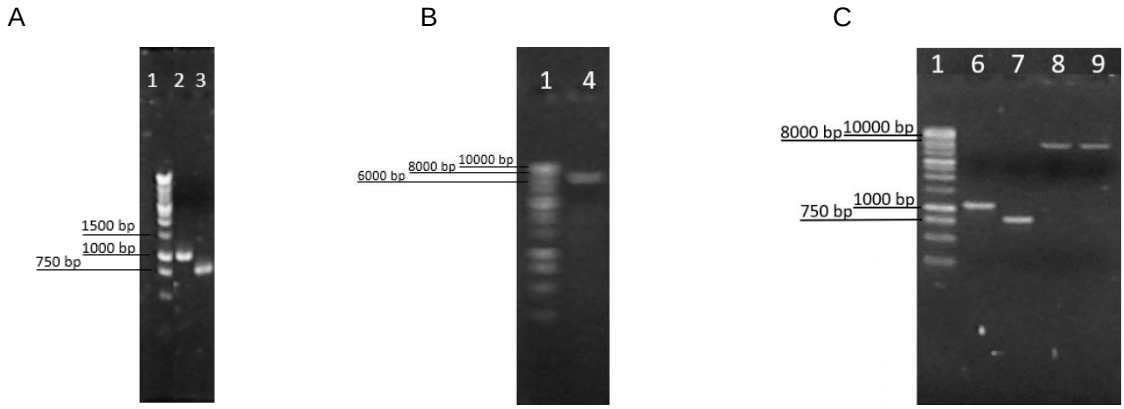

Figure 3.5 – Digested fragments and plasmids obtained for the construction of pBASE6-*hmp* and pBASE6-erm/lox1 and 2-*hmp* plasmids (A) Fragment A (2, 1142 bp, EcoRI/ XmaI) and B (3, 855 bp, XmaI/ EcoRV) and (B) pBASE6 plasmid (4, 6553 bp, EcoRI/Eco RV), for the construction of pBASE6-*hmp*. (C) Fragment A (6, 1144 bp, SalI/ NheI) and B (7, 851 bp, SacI and EcoRI) and pBASE6-erm/lox1 (8, 7864 pb, SalI/ NheI), and pBASE6-erm/lox2 (9, 7864 pb, SalI/ NheI) plasmids, for the construction of pBASE6-erm/lox1-*hmp* and pBASE6-erm/lox2-*hmp*. The electrophoresis was performed in 1% agarose gel in TAE buffer, at 80V, 400 mA for 40 minutes .1 Kb ladder (lane 1) was used as marker.

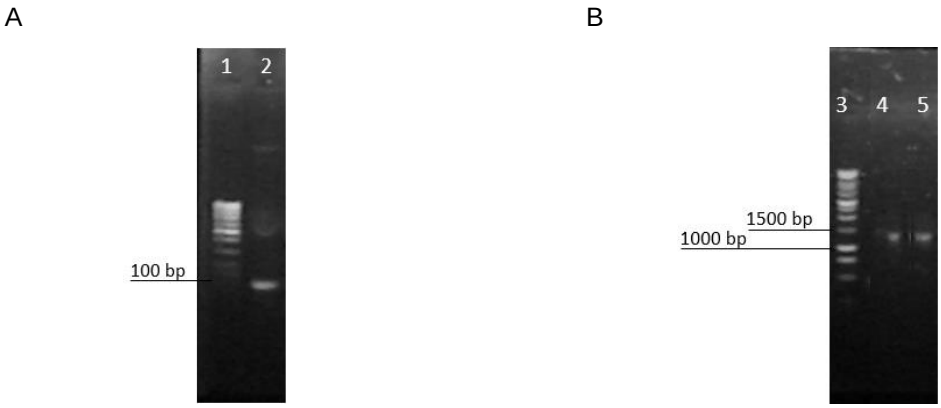

Figure 3.6 – PCR products obtained using the extracted pBASE6 plasmids and the pBASE6_fw and pBASE6_rev primers of pBASE6. (A) Lane 1, 100 bp ladder; lane 2, amplified product from pBASE6 (96 bp). (B) Lane 1, 1 kb ladder; lane 4 and 5, amplified products from pBASE6-erm/lox1 (1376 bp) and pBASE6-erm/lox2 (1376 bp), respectively.

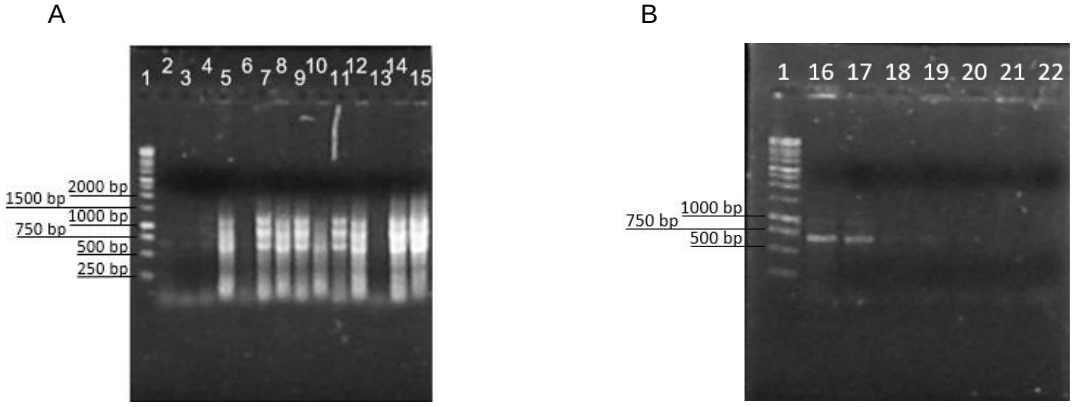

Figure 3.7 – Screening of *E. coli* DC10B colonies transformed with pBASE6 plasmids. PCR products obtained from colonies PCR on (A) 14 out of 42 colonies tested for the presence of pBASE6-*hmp* plasmid (expected size of 2050 bp) (lanes 2 to 15) and (B) 7 out of 27 for the pBASE6-erm/lox1-*hmp* and pBASE6-erm/lox2-*hmp* plasmids (3351 pb predicted fragments). The electrophoresis was performed in 1% agarose gel in TAE buffer, 80V, 400 mA for 40 minutes and ran with a 1 kb ladder marker (lane 1).

To bypass possible ligation problems, an attempt was made to create the A*erm*BB fragment via SOE-PCR[108]. The expected fragment (3306 bp) was obtained, however, extra bands were seen on the gel (Fig. 3.8A), which led us to successfully extract the fragment of interest (Fig. 3.8B) from the gel using a silica spin column, most applied for gel extraction[106]. This line of work could not be completed at the time but will be continued in the future.

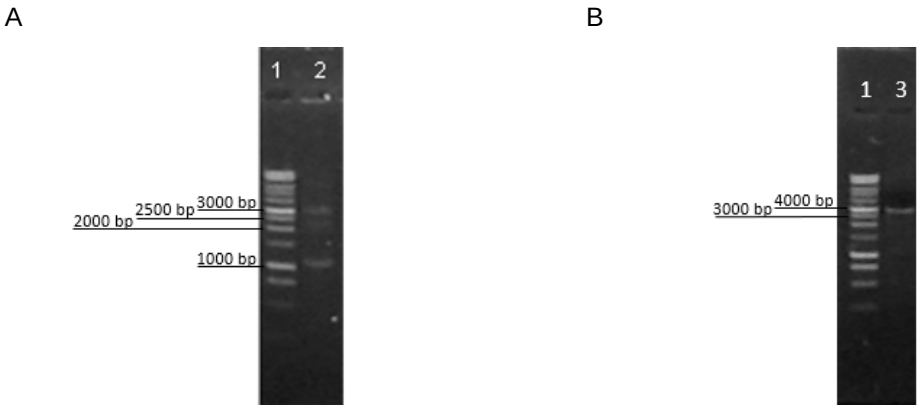

Figure 3.8 – PCR products obtained from SOE-PCR with A, ermB and B fragments. (A) SOE-PCR products (lane 2). (B) purified AermBB fragment (lane 3, 3306 pb). The electrophoresis was performed in 1% agarose gel in TAE buffer, at 80 V, 400 mA for 40 minutes. Lane 1, 1Kb ladder.

3.3 *Staphylococcus epidermidis* biofilms exposed to nitrosative stress

The effect of NO in *S. epidermidis* biofilms was studied in three strains, namely 1457, RP62A, and 1457-M12. The strains 1457 and RP62A are both strong PIA and biofilm producers, isolated from severe biofilm-catheter infections[12,13]. The mutant 1457-M12, also referred in this work as M12, is described as being a low PIA and biofilm producer[96]. M12 has a biofilm phenotype that resembles that of non-virulent skin commensal isolates, which typically lack the *icaADBC* genes[22,109], coding for PIA, which is the main exopolysaccharide produced by *S. epidermidis*[2].

All the strains were grown for 48 h on DMEM+FBS, a physiological medium widely used for the maintenance and growth of animal cells, including the macrophages of the innate immunity[110,111], and exposed to 1 mM DETANONOate. Due to the characteristics of DETANONOate, *i.e.*, half-life of 20h at 37ºC and pH 7, NO was produced over the time of biofilm formation as attested by nitrite quantification (data not shown). For comparison purposes, biofilms grown on TSB, the preferred medium for growth of staphylococci *in vitro*[112], and exposed to NO, were also analyzed.

3.3.1 TSB

In TSB and in the absence of NO, 1457 and RP62A strains produced similar biofilm amounts (around 2.5 of Abs_{590}), 2-fold higher than those of 1457-M12 strain (Fig. 3.9A). Nevertheless, the viability of biofilm cells (Bc) of 1457 and RP62A strains was 4- and 7-fold higher than that of 1457-M12 strain (p-value < 0.001), respectively (Fig. 3.9C). These data may result from higher amounts of matrix polymers, to which crystal violet binds, per biofilm in M12 and/or the presence of significant amounts of dead cells in M12 biofilms. In accordance with the first hypothesis, our results show that M12 biofilms contained significantly more proteins than 1457 and RP62A biofilms (*circa* 2.8- and 3.9- fold, p-value <0.01) (Fig. 3.9E). Since eDNA, which has been described as a minor component of biofilm EPS[113], derives from dead cells[2] future determinations of this polymer will be performed.

Thus, we show that although being a PIA underproducing strain, M12 compensates for its inability to synthesize PIA by increasing considerably the production of protein per biofilm cells[88,114]. Indeed, *ica* negative *S. epidermidis* isolates tend to have higher amounts of proteins in the biofilm[115].

Interestingly, the number of viable biofilm-released cells (BRc) of 1457 and 1457-M12 strains was significantly higher than that of the biofilms *per se* (about 1.7 and 8-fold, respectively), suggesting dispersion of cells from the biofilms at this stage (48 h of growth). Although the same tendency was observed for the RP62A strain, the difference was not statistically significant (*p*-value > 0.05) (Fig. 3.9C). In agreement with these results, it has been observed that the proportion of detached cells relative to biofilm-encased cells is smaller for thicker biofilm-producing strains[116].

In TSB and in the presence of NO, the total biofilm of strains 1457 and RP62A decreased significantly relative to untreated cells (Fig. 3.9A). Nevertheless, this effect was more accentuated for RP62A (2.6-fold decrease) than for 1457 (1.6-fold decrease), which can be in part explained by the decrease of the viability of RP62A biofilm cells exposed to NO, which was not observed for 1457 (Fig. 3.9C). In accordance, is the observation that RP62A, grown in TSB and exposed to *S*-nitroso-*N*-acetylpenicillamine (SNAP), an NO donor, show a major decrease in viability[117].

Interestingly, the total biofilm of strain 1457 exposed to NO dropped to values close to those of its isogenic mutant M12. Moreover, the M12 biofilm biomass remained unaltered by NO (Fig. 3.9A). These data suggest that the mutation in 1457-M12 of the *purR,* a gene regulator of purine synthesis shown to indirectly affect eDNA production[118] and *ica* genes expression under specific conditions[119], may have a role in *S. epidermidis* resistance to nitrosative stress. Accordingly, in *E. coli*, the *purR* operon was found to be repressed in the presence of NO[120].

In what concerns the effect of NO on the production of the matrix polymers of the biofilms, we show that NO inhibited significantly the accumulation of proteins and/or exopolysaccharides in the three strains (Fig. 3.9E). In line with these observations, inhibition of PIA synthesis by nitrites has been described in *S. aureus*[55]*.* As a consequence, NO led to a decrease in total biofilm of the strains 1457 and RP62A relative to control (Fig. 3.9A). However, this was not the case of M12 strain. Since the viability of 1457-M12 was not affected by nitric oxide (Fig. 3.9C), this discrepancy can be explained by differences in the amounts of dead cells and/or eDNA[117,121], to be determined in the continuation of this work.

Interestingly, the effect of nitric oxide on the viability of biofilm released cells did not always exhibit the same pattern as that observed for Bc (Fig. 3.9C). This is coherent with previous findings which report that biofilm released cells, present in the supernatant, have an intermediary phenotype between planktonic and biofilm cells, reflected, for example, in antibiotic resistance[122,123]. Biofilm-independent protection mechanisms of staphylococci against nitrosative stress have been previously described[57]. However, to our knowledge, no studies have been made on BRc response to NO.

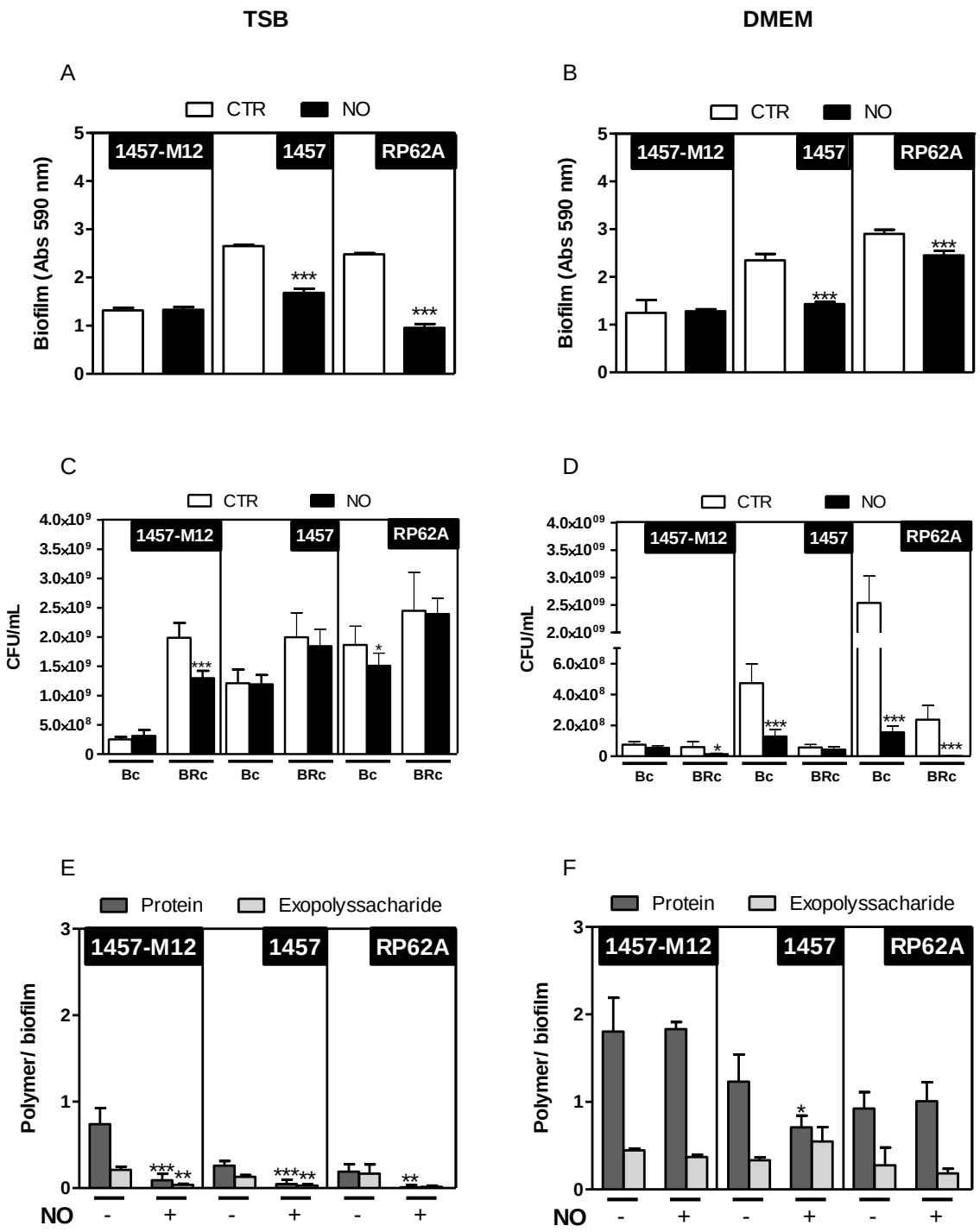

Figure 3.9 – Biofilm amounts, viability and EPS composition in *S. epidermidis* exposed to NO. Biofilms of 1457, 1457-M12 and RP62A strains were grown for 48h in TSB (A,C,E) and DMEM+FBS (B,D,F) and exposed to 1mM DETANONOATE. Total biofilm (A, B) was measured by crystal violet staining and absorbance at 590 nm, n≥8. Cell viability (C, D) in the biofilm encased (Bc) and released cells (BRc), in colony forming units (CFU)/mL, n≥2. Amount of each polymer (protein or exopolysaccharide) per total amount of biofilm (E, F) determined by sodium periodate and proteinase K treatments, respectively, n≥3. Statistical analysis was performed using two-tailed unpaired t-tests with a 95% confidence interval. Asterisks represent statistical significance of data by comparison with the control; *P<0.05, **P<0.01 and ***P<0.001.

3.3.2 DMEM+FBS

When grown in DMEM+FBS and without NO stress for 48 h, 1457 and RP62A strains formed similar biofilm amounts (Fig. 3.9B), which were about 2-fold higher than those formed by the M12 strain (*p*-value<0.001) (Fig. 3.9B), a pattern similar to that observed for the TSB-grown biofilms (Fig. 3.9A). In agreement, it has been described that PIA independent biofilms are weaker than the ones containing this exopolyssacharide[115]. Interestingly, the number of viable Bc 1457 and RP62A cells was significantly higher than that of viable BRcs (*p*-value<0.001) (Fig. 3.9D), which indicates less dispersion or detachment of biofilm cells to the surrounding medium when comparing with TSB-grown biofilm cells. Accordingly, the dispersion process was shown to be influenced by nutrient availability and the media used[123]. The total cell viability also showed great variability among the three strains, being higher for RP62A and lower for M12. These differences in the cell viability between the strains may be attributed to the presence of dead cells, an issue that requires further detailed analysis.

Regarding the EPS matrix composition, for all strains, the protein levels per biofilm after 48 h of growth were *circa* 3 times higher than the levels of exopolysaccharides (Fig. 3.9D). Moreover, after 48 h, we observed a significant depletion of glucose and other nutrients in the medium surrounding the biofilms (data not shown). These results are in line with the observation that nutrient-limited environments inhibit PIA production[32,124]. Furthermore, protein and exopolysaccharide levels per biofilm were higher in strain M12 than in 1457 and RP62A strains, as also observed for biofilms formed in TSB.

When grown in DMEM+FBS and under NO stress, *S. epidermidis* 1457 and RP62A revealed a significant decrease in total biofilm amount, which was not observed for strain M12 (Fig. 3.9B). Interestingly, this decrease was considerably lower than that observed for the biofilm cells viability in the presence of NO (about 3.9-fold for 1457 and 16-fold for RP62A) (Fig. 3.9D). As for the amounts of the matrix polymers of the biofilms exposed to NO, there was no change in RP62A and for the 1457 strain, a significant decrease of the protein content per biofilm was observed (Fig. 3.9E). In general, these results indicate the presence of dead cells in the biofilms of 1457 and RP62A strains. Altogether, we conclude that NO kills biofilm cells of 1457 and RP62A strains and inhibits protein accumulation in the EPS of the 1457 biofilms (Fig. 3.9). Moreover, the alteration of the 1457 matrix caused by NO was visible during the manipulation of strain 1457 in the laboratory (Fig. 3.10B). In the absence of NO, 1457 strain biofilms formed aggregates of difficult resuspension but loose from the bottom of the plate wells. However, when grown with NO, the 1457 biofilms became easier to homogenize, showing a phenotype closer to the one observed for M12 (with and without NO). In turn, RP62A biofilms were very attached to the wells but, once removed, easily resuspended in buffer (Fig. 3.10).

Unlike the 1457 WT, the protein content of the EPS of 1457-M12 was not affected by nitrosative stress (Fig. 3.9F). This was an intriguing result that might be explained by the effect of the mutation of *purR,* on the protein content, of M12. For instance, the expression of proteins, such as Aap and Bhp, is known to impact the surface charge and hydrophobicity of the bacteria, thus altering

their capacity to adhere to surfaces, form biofilms, and resist antimicrobials[115]. To understand the protective effect of the M12 biofilm against NO, the expression of biofilm proteins in cells treated and untreated with NO will be analyzed in future studies.

A B C

Figure 3.10 – Picture showing biofilms of *S. epidermidis* strains 1457-M12 (A), 1457 (B) and RP62A (C) grown in DMEM+FBS, in 24 well plates for 48h, exposed or not to NO and then resuspended in PBS.

Overall, our data showed that, albeit differently and dependent on the media, the cell viabilities of all the tested *S. epidermidis* strains, were affected by nitrosative stress. In both media, the presence of NO did not affect the total biofilm of M12, whereas it significantly decreased the amounts of 1457 and RP62A, the strong biofilm producers. Total biofilm reductions were shown to be caused by the effect of NO in the amounts of different EPS components, according to the growth media. Previously, it was demonstrated that the growth media influences biofilm formation and resistance to stressors in *S. epidermidis*[125–128]*.* In the presence of NO, alterations in protein and exopolysaccharide of the matrix were prominent when grown in TSB, while variations of the viability were higher in DMEM+FBS. Exceptionally, when *S. epidermidis* was grown in DMEM media, EPS protein declined significantly, with the addition of nitric oxide, in strain 1457. Finally, M12 biofilms revealed to be less susceptible to NO when referring to the analyzed characteristics, than their wild type counterparts, possibly due to a *purR* mutation, and consequent alteration in the protein content of the biofilm. Nevertheless, future analysis of the biofilm content, including eDNA and dead cells quantification and identification of the different exopolysaccharides and proteins is required to clarify the effect of NO in the biofilm.

3.4 Quantification of extracellular metabolites in DMEM-grown *S. epidermidis biofilms*

Metabolic studies of bacteria require a media with clearly defined chemical compositions. DMEM, unlike the rich TSB, is a medium with a well-defined composition and with low concentrations of paramagnetic ions, thus being suitable to grow bacteria for NMR studies. Moreover, DMEM+FBS is considered to resemble the nutritional environment encountered by bacteria in the human body[110]. Therefore, to elucidate how *S. epidermidis* M12, 1457 and RP62A biofilms sustain nitrosative stress, they were grown in DMEM+FBS for 48 h in 24-well plates and exposed to 1 mM DETANONOate, and their metabolic state was studied by ^{1}H-NMR quantification of glucose consumption and excreted end

products (Fig. 3.11). For that, supernatants from biofilms exposed and unexposed to NO were treated with methanol to precipitate FBS and stored for further analysis.

After 48 h of growth of each strain without NO addition, all glucose was consumed (data not shown). Moreover, the increased amounts of produced lactate when compared to acetate (Fig. 3.11A,B) indicates that the three strains present a fermentative metabolism for energy production[129], consistently to what has been described in staphylococci biofilms[130,131]. Lactate, acetate, and formate were ubiquitously present in the extracts of the three strains (Fig. 3.11), indicating the presence of activated LDH, PTA, AK, and PFL, and have already been described as fermentation products of the metabolism of *S. aureus* grown under fermentative conditions[129].

The values of consumed glucose normalized per biofilm varied among the studied *S. epidermidis* strains, being significantly higher for 1457-M12, the PIA underproducing strain, than for the strong biofilm producers, *i.e*. 2- and 2.9-fold higher than the values obtained for 1457 and RP62A, respectively (Fig. 3.11A). The same trend was observed for the accumulation of extracellular lactate and acetate (Fig. 3.11B). Although in smaller quantities, excreted formate and succinate were also measured. Accordingly, lactate was previously described, in *S. aureus,* to be the major product of glucose catabolism in anaerobic conditions[132]. Interestingly, M12, the PIA defective mutant exported the higher amount of lactate, which can be translated into a higher activity of lactate dehydrogenase[133], followed by 1457 and finally RP62A (Fig. 3.11A). Increased activity of LDH was correlated with decreased total biofilm amounts (Fig. 3.9B). The higher activity of LDH in 1457-M12 may be correlated to its deficient PIA synthesis, as fructose 6-phosphate is not diverted to N-acetylglucosamine synthesis, and thus is available to complete glycolysis and enter lactic acid fermentation. Finally, higher fermentation products per biofilm are also associated with a greater content of protein per biofilm (Fig. 3.9F), as ATP is needed to produce these exopolymeric substances. In conditions where bacteria need to grow biofilms, ATP is diverted to this goal, even at the expense of growth rate[131]. Furthermore, strains with greater biofilm amounts may have a higher percentage of persister cells, defined by being less metabolically active[134]. For example, biofilms of RP62A can contain up to 94% of persister cell when in stationary phase, under stress conditions[135].

Succinate was lower in RP62A, followed by 1457 and M12, following the same trend as lactate, glucose consumption and protein amounts in the biofilm (Fig. 3.11C). Accordingly, it is described that greater production of succinate is correlated with increased tricarboxylic acid cycle activity, associated with glucose depletion, and a more proteinaceous biofilm[28]. Formate, however, was found in lower quantities in 1457 than in M12 and RP62A (Fig. 3.11C). These data suggest a decreased activity of the pyruvate formate lyase of 1457 when compared with 1457-M12 and RP62A (Fig. 3.12).

Accumulation of acids produced by fermentation (Fig. 3.11) lowered the pH of the media, as attested by the change of color of the phenol red indicator present in the DMEM media. These molecules can contribute to EPS environment acidification, which has a stabilizing effect, as the proteins present have a high pI and thus in acidic environment become positively charged, promoting

interactions with eDNA and negatively charged extracellular metabolites and surface cell components[26].

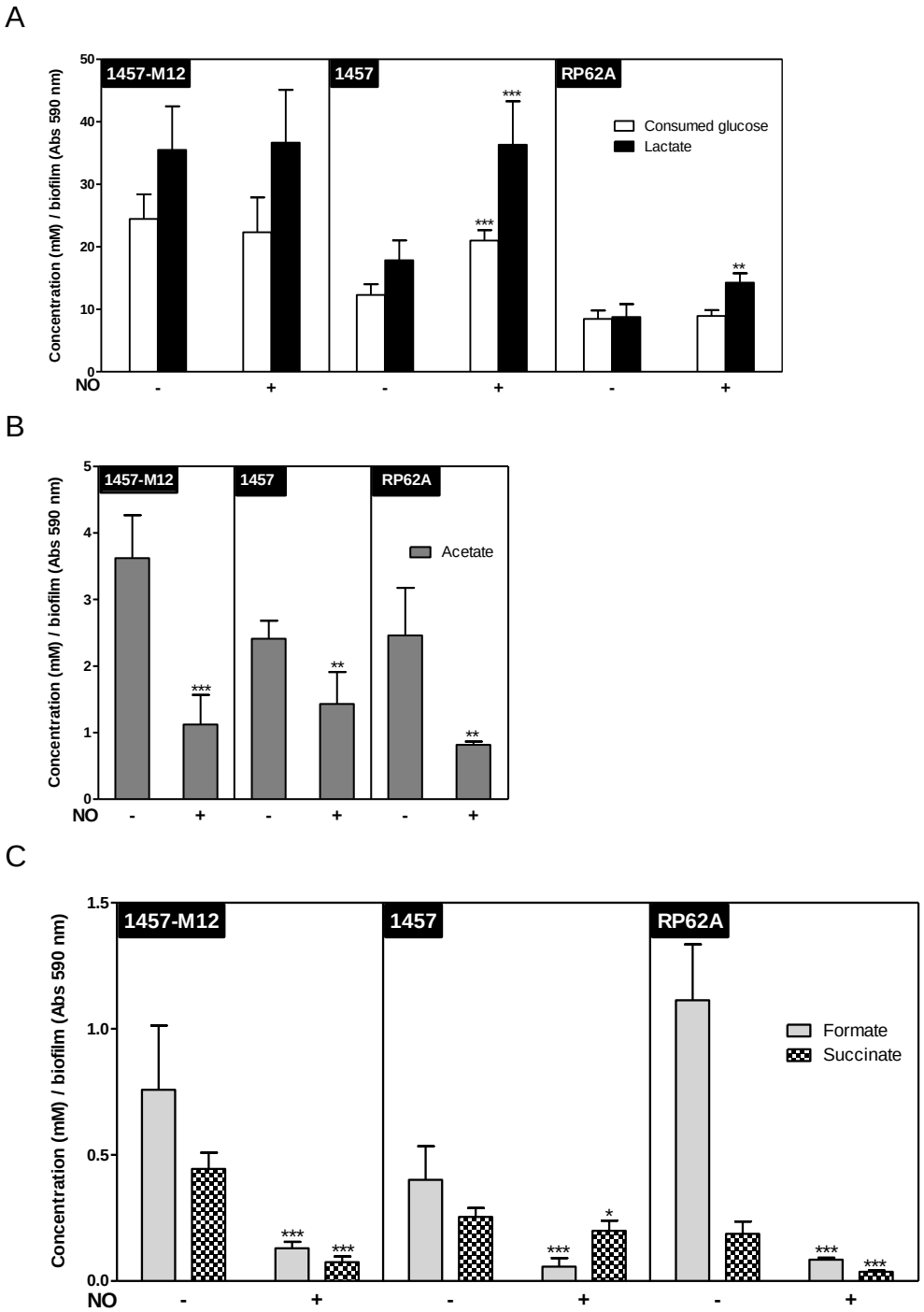

Figure 3.11 – Quantification, by ^{1}H-NMR analysis, of extracellular metabolites produced by *S. epidermidis* 1547-M12, 1457, and RP62A, grown in DMEM. Amounts of consumed glucose (A), and produced lactate (A), acetate (B), formate and succinate (C) were measured. Averages and standard deviations with a minimum of three independent replicates performed in duplicate are shown. Statistics was made using two-tailed unpaired t-tests with a 95% confidence interval. Asterisks represent statistical significance of data by comparison with the control; *P<0.05, **P<0.01 and ***P<0.001.

The addition of NO to the growth media led to increased production of lactate in strain 1457 and RP62A (*circa* 2- and 1.6-fold, respectively) relative to untreated cells (Fig. 3.11A), however, all the strains, produced significantly less acetate, formate, and succinate (Fig. 3.11).

In 1457 and RP62A biofilms exposed to NO, an increase in extracellular lactate accumulation in biofilms was observed suggesting an increased activity of LDH. Our observations are supported by previous measurements (qRT-PCR), in our lab, of *ldh* expression, which was shown to be increased with nitrosative stress in 1457 grown in DMEM (data not shown). Moreover, the lactate increase in the presence of nitrosative stress had already been described for planktonic *S. aureus*[59], and fermentation was shown to facilitate growth under nitrosative stress by contributing to the redox balance through the conversion of NADH into NAD^{+}[136].

Curiously, 1457-M12 produced a similar amount of lactate with or without NO, values equated by 1457 under nitrosative stress (Fig. 3.11A), which is representative of an increased activity of LDH. Total biofilm amounts followed an inverse trend when compared to lactate amounts, *i.e.* under NO stress total biofilm amounts decreased significantly in strains 1457 and RP62A, but not in M12 (Fig. 3.9A). This tendency was also observed among the strains not subjected to NO (Fig. 3.9A) and reiterates the hypothesis that the biofilm amount is deeply connected with the fermentative activity of the cell. The connection between increased lactate production and the effect of NO on the biofilm matrix and viability may be mediated by SrrAB, a regulator expressed by *S. epidermidis* that is involved in biofilm formation[137]. Indeed, we observed a correlation between increased lactate and decreased succinate production. The inferred increase in LDH upregulation and TCA cycle downregulation was previously described through proteomic data, in anaerobically grown *S. aureus,* to be co-regulated by SrrAB[129].

Extruded succinate decreased in significant amounts, in all the strains, when exposed to NO (Fig. 3.11C), which indicated a decrease in the TCA cycle activity. TCA inhibition may result from decreased acetyl-CoA availability, as indicated by a decrease in formate and acetate amounts[129], products of pyruvate formate lyase and pyruvate dehydrogenase, enzymes whose reactions also produce acetyl-CoA (Fig. 3.12). In fact, nitric oxide inhibits the activity of pyruvate dehydrogenase in *S. epidermidis*[59] and, in *S. aureus*, acetate accumulation is lower[58] and these enzymes are downregulated by NO, limiting the production of acetyl-CoA[136].

In short, *S. epidermidis* biofilms main energy production happens through fermentation, even though with differences among strains. Nitric oxide effects on lactate production can be correlated with biofilm production as alterations are seen in 1457 and RP62A but not in M12. However, the effect of NO on formate and acetate production, and the TCA cycle was consistent in all the strains, suggesting these processes are independent of the M12 mutation.

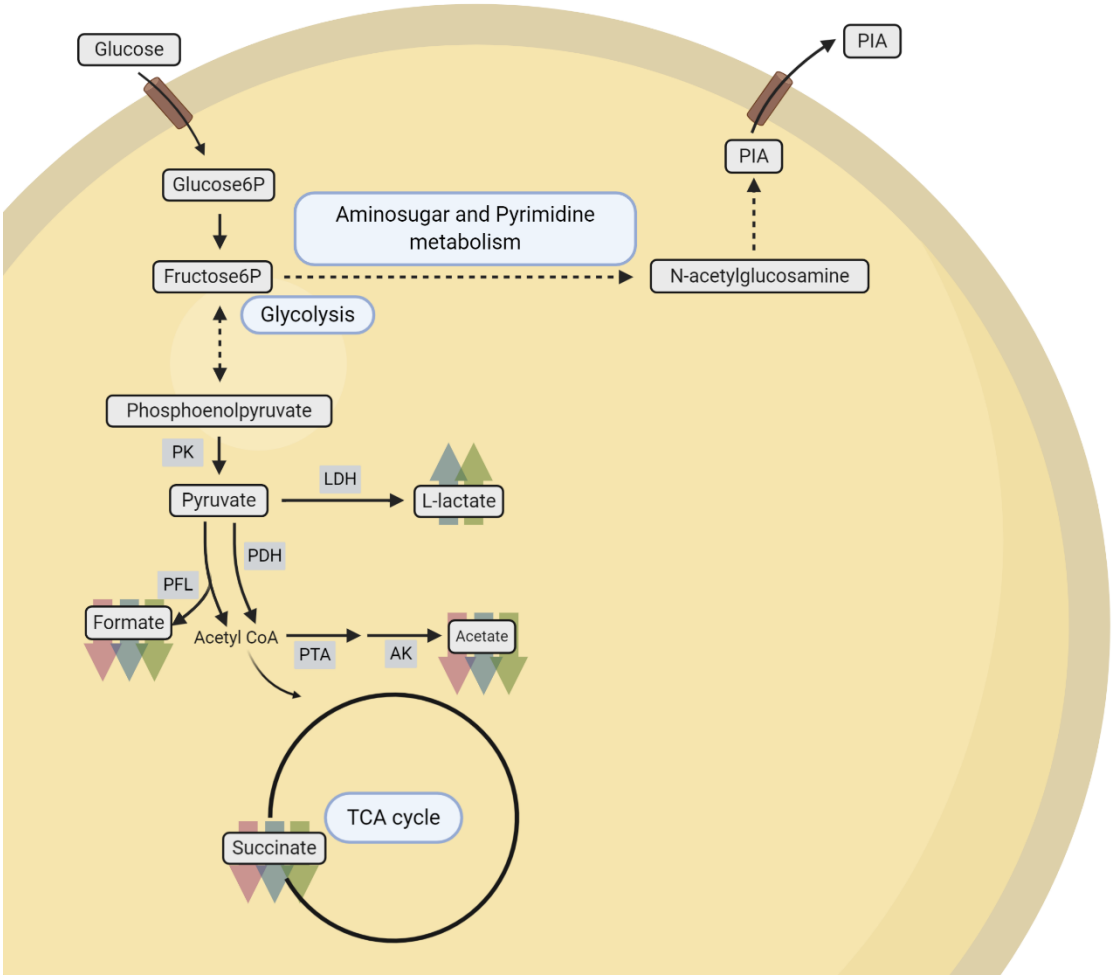

Figure 3.12 – Schematic representation of metabolites affected by nitrosative stress and related pathways. Arrows represent metabolite concentration variation (↑increase and ↓decrease) in each of the *Staphylococcus epidermidis* analyzed strains (1457-M12 in pink, 1457 in blue, and RP62A in green). PK- pyruvate kinase; PDH - pyruvate dehydrogenase; LDH - lactate dehydrogenase; PFL - pyruvate formate lyase; PTA - phosphate acetyltransferase; AK - acetate kinase. Image created by the author of this thesis, Ana Rita Oliveira in BioRender.

3.5 Optimization of intracellular metabolites extraction from *S. epidermidis* biofilms

To further elucidate the metabolic behavior of biofilms exposed to NO, and its impact on biofilm viability and matrix composition, attempts were made to create a protocol for intracellular metabolites extraction, such as PIA and matrix proteins precursors, in *S. epidermidis*, as, to our knowledge none is available in the literature.

Intracellular metabolites exist in a wide and dynamic chemical range[138] and, therefore, several aspects, such as pH, temperature, correct separation of the cells from the culture media, washing procedures and solutions, quenching times and reagents, and cell lysis reagents, their polarity and metabolite degradation, must be considered when designing an extraction protocol[138–140].

Methods for the extraction of phosphorylated metabolites were used, as we intended to analyze the impact of NO in the metabolism of the TCA cycle, glycolysis, and aminosugar pathways, rich in these molecules. The metabolite extraction protocols tested included filtration, and two different sonication conditions, along with freezing in liquid nitrogen and solutions of methanol, chloroform, and ammonium hydroxide. Methanol (-20ºC) and a mixture of methanol and chloroform are very commonly used as quenching and extraction solutions, respectively[141]. Methanol is a polar solvent, used for the extraction of small organic molecules, and chloroform is used for the extraction of hydrophobic metabolites. Together, they amount to a high concentration of organic solvents which aids in the precipitation of macromolecules such as proteins and nucleic acids[138,141,142].

Method **1.**, the use of a combination of methanol and chloroform for metabolite extraction, did not result in observable metabolites in the cell extract (Fig. 3.13A), possibly due to inappropriate cell disruption. Authors previously describing similar methods also showed concern that there could be a metabolic profile alteration as a consequence of the filtration time, especially in quickly metabolized molecules, such as phosphorylated compounds,[75,143] and possible metabolite leakage due to the saline solution used in the washing steps[144]. This ought to be tested in every protocol by NMR analysis of the washing solution. Ammonium hydroxide was added in method **2.** (Fig. 3.13D) as it can be used as a pH regulator to avoid that some metabolites dissolve in the chloroform phase and is compatible with downstream applications as mass spectrometry[149]. This addition somehow improved the results but not significantly, suggesting the need to improve cell disruption. For the next methods tested, sonications were added to the methanol and chloroform extraction in order to improve cell disruption (Fig. 3.13C,D). Method **3.** contained a cell disruption step via a bath sonicator, whereas method **4.** involved a probe sonicator. Sonication as a disruption method to extract intracellular metabolites has been previously proven efficient[77]. These methods appear to have been able to disrupt the cells to an extent, as some peaks can be seen on the NMR spectra, although with varying noise levels and showing too few peaks to possibly represent all the metabolites present in the cell[145–148], suggesting that these methods may be degrading or not properly extracting the metabolites. The alteration of the extracted metabolic profile by degradation can happen due to sonication as it can hydrolyze macromolecules as nucleic acids, proteins, and polysaccharides into detectable metabolites[138] which can translate into some of the peaks visible in the NMR spectra. Metabolite degradation will be analyzed in the future, to aid in the optimization of protocols, by adding substances in known concentrations to the cells, before extraction, and later quantifying them by NMR

Although the most suitable method for intracellular metabolite extraction from *Staphylococcus epidermidis* biofilms was not yet attained, based on these results, successful optimization is expected.

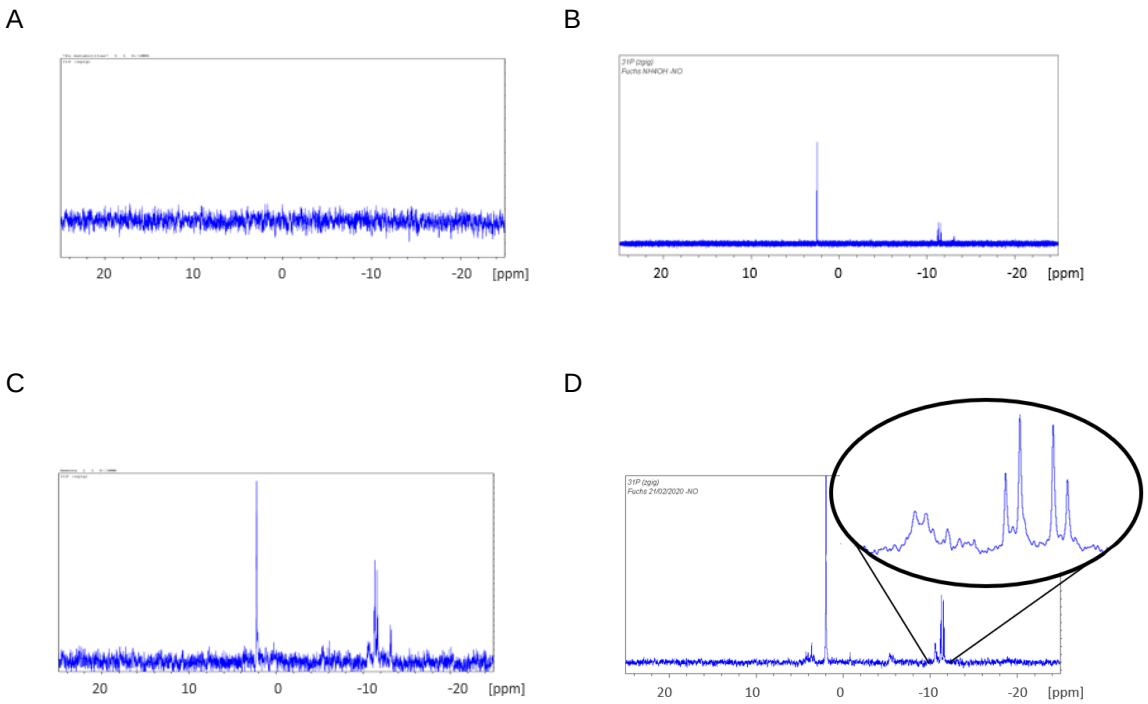

Figure 3.13 – ^{31}P-NMR spectra resulting from different methods of metabolites chloroform and methanol extraction based on filtration (A, method **1.**); addition of ammonium hydroxide (D, **2.**); and centrifugation coupled with sonication (B and C, **3.** and **4.**).

.

4 Conclusions

Staphylococcus epidermidis is often the cause of nosocomial and indwelling medical devices related infections, being one of the most frequent pathogens involved in bacteremia and sepsis. The pathogenicity of this microorganism is deeply connected with the formation of biofilms, which confer resistance to the immune system of the host. Nitric oxide, a molecule produced by innate immune cells, has been shown to disrupt *S. epidermidis* biofilms. However, there is a general lack of knowledge on how *S. epidermidis* resists NO.

In this work, we studied the impact of NO on *S. epidermidis* biofilms by determining the viability and the total amount of biofilm and matrix polymers produced, under stress conditions, by 1457 and RP62A, two clinical strains that form strong biofilms, and 1457-M12, a biofilm underproducing strain with phenotypic resemblance to commensal strains. Moreover, we also analyzed how the metabolism of the *S. epidermidis* strains adapts and responds to nitrosative stress.

Overall, we show that nitric oxide inhibited significantly the formation of 1457 and RP62A biofilms, but not that of M12, suggesting that PIA underproducing strains and clinical strains have a distinct behavior when exposed to NO. Moreover, the decrease in the total biofilm amounts in 1457 and RP62A strains by NO was dependent on the strain and growth media.

Our metabolite profiling data shows that in DMEM-grown *S. epidermidis* biofilms, NO inhibited the extracellular accumulation of acetate, formate, and succinate, suggesting inhibition of acetate kinase, pyruvate formate-lyase, and TCA cycle activities, respectively. Moreover, the results indicated that the resistance of strong biofilm producers, such as 1457, to NO is achieved through increased activity of glycolysis and lactate dehydrogenase. Furthermore, we unveiled a subtle interplay between lactate production or lactate dehydrogenase activity and biofilm amounts. We propose that exposure to NO of *S. epidermidis* PIA producing strains decreases cell viability and triggers glycolysis and lactate dehydrogenase activity, that results in lower production of matrix PIA exopolysaccharide and/or proteins, and consequently, lower biofilm amounts. In M12, a PIA underproducing strain, lactate dehydrogenase was shown to operate at high activity, as indicated by lactate amounts, independently of the presence of NO, which reflected in unchanged biofilm amounts.

Further studies, such as intracellular metabolites and PIA quantifications, are required to confirm and complement the data obtained in this work

Exploring the mechanisms that integrate biofilm matrix formation and lactate production, glycolysis, and other central metabolic pathways will certainly contribute to an improved understanding of what is controlling biofilm formation.

5 Future Work

The work presented in this master thesis contributed to the advance of the knowledge of the effect of nitric oxide on *Staphylococcus epidermidis* biofilms. We observed an alteration in matrix protein and exopolysaccharide contents due to nitrosative stress, however, it was not clear which molecules were affected and which pathways mediated the effect. Thus, in the future, it would be of great interest to analyze by real-time PCR the expression of potential target genes, focusing on pathways involved in matrix protein and exopolysaccharide production and the central metabolism, related to glucose, lactate, acetate, formate, and succinate synthesis, as these metabolites were revealed to be altered by NO. A direct quantification of the biofilm components would also be necessary, in order to confirm the results, as well as the quantification of eDNA and death cells in the biofilm.

Persisters and biofilm released cell are often associated with resistance to antibiotics and the immune system, and colonization of different infection sites, respectively. Therefore, the metabolomics analysis of persister and biofilm released cells may also be of interest to better understand the dynamics of nitric oxide response by the different types of cells present in an infection scenario.

Part of this thesis shows the development of protocols for *S. epidermidis.* Consequently, the optimization must be continued to achieve the goals of studying the possible protective role of *S. epidermidis* Hmp against nitrosative stress and completing the metabolic data with intracellular metabolites analysis. Different methods may be tested for the construction of mutants, as transposon mutations or phage technology. A protocol for the extraction of intracellular metabolites from *S. epidermidis* biofilms needs to be optimized, and for that several quenching and extraction procedures and degradation tests will be performed.

Finally, to complete the information and validate the obtained results in the context of infection, experiences with *S. epidermidis* biofilms *ex vivo* (with macrophages) and *in vivo* (with mice) would be also highly relevant.

6 References

1. Otto M. Molecular basis of *Staphylococcus epidermidis* infections. *Semin Immunopathol*. 2012;34(2):201-214. doi:10.1007/s00281-011-0296-2
2. Otto M. Staphylococcal Biofilms. *Microbiol Spectr*. 2018;6(4):1-17. doi:10.1128/microbiolspec.GPP3-0023-2018
3. Speziale P, Pietrocola G, Foster TJ, Geoghegan JA. Protein-based biofilm matrices in staphylococci. *Front Cell Infect Microbiol*. 2014;4(NOV):1-10. doi:10.3389/fcimb.2014.00171
4. Kleinschmidt S, Huygens F, Faoagali J, Rathnayake IU, Hafner LM. *Staphylococcus epidermidis* as a cause of bacteremia. *Future Microbiol*. 2015;10(11):1859-1879. doi:10.2217/fmb.15.98
5. Otto M. *Staphylococcus epidermidis* - the 'accidental' pathogen. *Nat Rev Microbiol*. 2009;7(August). doi:10.1038/nrmicro2182
6. Oliveira WF, Silva PMS, Silva RCS, et al. *Staphylococcus aureus* and *Staphylococcus epidermidis* infections on implants. *J Hosp Infect*. 2018;98(2):111-117. doi:10.1016/j.jhin.2017.11.008
7. Rohde H, Frankenberger S, Zähringer U, Mack D. Structure, function and contribution of polysaccharide intercellular adhesin (PIA) to *Staphylococcus epidermidis* biofilm formation and pathogenesis of biomaterial-associated infections. *Eur J Cell Biol*. 2010;89(1):103-111. doi:10.1016/j.ejcb.2009.10.005
8. Rupp ME. Clinical characteristics of infections in humans due to *Staphylococcus epidermidis*. In: Fey PD, ed. *Staphylococcus Epidermidis Methods and Protocols*. Omaha , NE, USA: Humana Press; 2014:1-16. doi:10.1007/978-1-62703-736-5
9. Lee JYH, Monk IR, Gonçalves da Silva A, et al. Global spread of three multidrug-resistant lineages of *Staphylococcus epidermidis*. *Nat Microbiol*. 2018;3(10):1175-1185. doi:10.1038/s41564-018-0230-7
10. Chabi R, Momtaz H. Virulence factors and antibiotic resistance properties of the *Staphylococcus epidermidis* strains isolated from hospital infections in Ahvaz, Iran. *Trop Med Health*. 2019;47(1):1-9. doi:10.1186/s41182-019-0180-7
11. Mack D, Siemssen N, Laufs R. Parallel induction by glucose of adherence and a polysaccharide antigen specific for plastic-adherent *Staphylococcus epidermidis*: Evidence for functional relation to intercellular adhesion. *Infect Immun*. 1992;60(5):2048-2057. doi:10.1128/IAI.60.5.2048-2057.1992
12. Gill SR, Fouts DE, Archer GL, et al. Insights on evolution of virulence and resistance from the complete genome analysis of an early methicillin-resistant *Staphylococcus aureus* strain and a biofilm-producing methicillin-resistant *Staphylococcus epidermidis* strain. *J Bacteriol*. 2005;187(7):2426-2438. doi:10.1128/JB.187.7.2426-2438.2005
13. Galac MR, Stam J, Maybank R, et al. Complete genome sequence of *Staphylococcus epidermidis* 1457. *Genome Announc*. 2017;5(22):15-17. doi:10.1128/genomeA.00450-17
14. Wadood A, Ghufran M, Khan A, et al. The methicillin-resistant *S. epidermidis* strain RP62A genome mining for potential novel drug targets identification. *Gene Reports*. 2017;8:88-93. doi:10.1016/j.genrep.2017.06.002
15. Knobloch JKMM, Bartscht K, Sabottke A, Rohde H, Feucht HH, Mack D. Biofilm formation by *Staphylococcus epidermidis* depends on functional RsbU, an activator of the sigB operon: Differential activation mechanisms due to ethanol and salt stress. *J Bacteriol*. 2001;183(8):2624-2633. doi:10.1128/JB.183.8.2624-2633.2001
16. Mack D, Sabottke A, Dobinsky S, Rohde H, Horstkotte MA. Differential expression of methicillin resistance by different biofilm-negative *Staphylococcus epidermidis* transposon mutant classes. *Society*. 2002;46(1):178-183. doi:10.1128/AAC.46.1.178
17. Polonio RE, Mermel LA, Paquette GE, Sperry JF. Eradication of biofilm-forming *Staphylococcus epidermidis* (RP62A) by a combination of sodium salicylate and vancomycin. *Antimicrob Agents Chemother*. 2001;45(11):3262-3266. doi:10.1128/AAC.45.11.3262-3266.2001
18. Oliveira D, Borges A, Simões M. *Staphylococcus aureus toxins* and their molecular activity in

infectious diseases. *Toxins (Basel)*. 2018;10(6). doi:10.3390/toxins10060252
19. Le KY, Park MD, Otto M. Immune evasion mechanisms of *Staphylococcus epidermidis* biofilm infection. *Front Microbiol*. 2018;9(FEB):1-8. doi:10.3389/fmicb.2018.00359
20. Brescó MS, Harris LG, Thompson K, et al. Pathogenic mechanisms and host interactions in *Staphylococcus epidermidis* device-related infection. *Front Microbiol*. 2017;8(AUG). doi:10.3389/fmicb.2017.01401
21. Davis SL, Gurusiddappa S, McCrea KW, Perkins S, Höök M. SdrG, a fibrinogen-binding bacterial bdhesin of the bicrobial burface components recognizing adhesive matrix molecules subfamily from *Staphylococcus epidermidis*, targets the thrombin cleavage site in the Bβ chain. *J Biol Chem*. 2001;276(30):27799-27805. doi:10.1074/jbc.M103873200
22. Fey PD, Olson ME. Current concepts in biofilm formation of *Staphylococcus epidermidis*. *Future Microbiol*. 2010;5(6):917-933. doi:10.2217/fmb.10.56.Current
23. Kanehisa M, Goto S. KEGG: Kyoto Encyclopedia of Genes and Genomes. *Nucleic Acids Res*. 2000;28(1):27-30. doi:10.1093/nar/28.1.27
24. Kanehisa M. Toward understanding the origin and evolution of cellular organisms. *Protein Sci*. 2019;28(11):1947-1951. doi:10.1002/pro.3715
25. Kanehisa M, Furumichi M, Sato Y, Ishiguro-Watanabe M, Tanabe M. KEGG: integrating viruses and cellular organisms. *Nucleic Acids Res*. 2020;Oct 30(gkaa970). doi:10.1093/nar/gkaa970
26. Graf AC, Leonard A, Schäuble M, et al. Virulence factors produced by *Staphylococcus aureus* biofilms have a moonlighting function contributing to biofilm integrity. *Mol Cell Proteomics*. 2019;18(6):1036-1053. doi:10.1074/mcp.RA118.001120
27. Arciola CR, Campoccia D, Ravaioli S, Montanaro L. Polysaccharide intercellular adhesin in biofilm: Structural and regulatory aspects. *Front Cell Infect Microbiol*. 2015;5(FEB):1-10. doi:10.3389/fcimb.2015.00007
28. Vuong C, Kidder JB, Jacobson ER, Otto M, Proctor RA, Somerville GA. *Staphylococcus epidermidis* polysaccharide intercellular adhesin production significantly increases during tricarboxylic acid cycle stress. *J Bacteriol*. 2005;187(9):2967-2973. doi:10.1128/JB.187.9.2967-2973.2005
29. Sadykov MR, Hartmann T, Mattes TA, et al. CcpA coordinates central metabolism and biofilm formation in *Staphylococcus epidermidis*. *Microbiology*. 2011;157(12):3458-3468. doi:10.1099/mic.0.051243-0
30. Arora S, Li X, Hillhouse A, et al. *Staphylococcus epidermidis* MSCRAMM SesJ is encoded in composite islands. *MBio*. 2020;11(1). doi:10.1128/mBio.02911-19
31. Pankov R, Kenneth M. Fibronectin at a glance. *J Cell Sci*. 2002;(115):3861-3863. doi:10.1242/jcs.00059
32. Zhu Y, Xiong YQ, Sadykov MR, et al. Tricarboxylic acid cycle-dependent attenuation of *Staphylococcus aureus* in vivo virulence by selective inhibition of amino acid transport. *Infect Immun*. 2009;77(10):4256-4264. doi:10.1128/IAI.00195-09
33. De Backer S, Sabirova J, De Pauw I, et al. Enzymes Catalyzing the TCA- and Urea Cycle Influence the Matrix Composition of Biofilms Formed by Methicillin-Resistant *Staphylococcus aureus* USA300. *Microorganisms*. 2018;6(4):113. doi:10.3390/microorganisms6040113
34. Zatorska B, Arciola CR, Haffner N, Lusignani LS, Presterl E, Diab-elschahawi M. Bacterial Extracellular DNA Production Is Associated with Outcome of Prosthetic Joint Infections. *Biomed Res Int*. 2018;2018. doi:10.1155/2018/1067413
35. Arciola CR, Campoccia D, Montanaro L. Implant infections: Adhesion, biofilm formation and immune evasion. *Nat Rev Microbiol*. 2018;16(7):397-409. doi:10.1038/s41579-018-0019-y
36. Pisithkul T, Schroeder JW, Trujillo EA, et al. Metabolic remodeling during biofilm development of *Bacillus subtilis*. *MBio*. 2019;10(3). doi:10.1128/mBio.00623-19
37. Freitas AI. *The role and the prevalence of icaABDC , aap and bhp genes in the virulence of Staphylococcus epidermidis Portuguese isolates*. Porto:Instituto de Ciências Biomédicas Abel Salazar da Universidade do Porto; 2015.
38. Loza-correa M, Ayala JA, Perelman I, et al. The peptidoglycan and biofilm matrix of *Staphylococcus epidermidis* undergo structural changes when exposed to human platelets. *PLoS One*. 2019;14(1):1-18. doi:10.1371/journal.pone.0211132
39. Yatim KM, Lakkis FG. A brief journey through the immune system. *Clin J Am Soc Nephrol*. 2015;10(7):1274-1281. doi:10.2215/CJN.10031014
40. Beutler B. Innate immunity: An overview. *Mol Immunol*. 2004;40(12):845-859.

doi:10.1016/j.molimm.2003.10.005
41. Dapunt U, Hänsch GM, Arciola CR. Innate immune response in implant-associated infections: Neutrophils against Biofilms. *Materials (Basel)*. 2016;9(5). doi:10.3390/ma9050387
42. Watters C, Fleming D, Bishop D, Rumbaugh KP. Host Responses to Biofilm. In: *Progress in Molecular Biology and Translational Science*. Vol 142. Elsevier B.V.; 2016:193-239. doi:10.1016/bs.pmbts.2016.05.007
43. Hänsch GM. Host Defence against Bacterial Biofilms: “Mission Impossible”? *ISRN Immunol*. 2012;2012:1-17. doi:10.5402/2012/853123
44. Schauber J, Gallo R. Antimicrobial peptides and the skin immune defense system. *J Allergy Clin Immunol*. 2008;23(1):1-7. doi:10.1038/jid.2014.371
45. Fang FC, Hazlitt W. Antimicrobial reactive oxygen and nitrogen species : concepts and controversies. *Nat Rev Microbiol*. 2004;2(October):820-832. doi:10.1038/nrmicro1004
46. Cinelli MA, Do HT, Miley GP, Silverman RB. Inducible nitric oxide synthase: Regulation, structure, and inhibition. *Med Res Rev*. 2020;40(1):158-189. doi:10.1002/med.21599
47. Bogdan C. Nitric oxide and the immune response. *Nat Immunol*. 2001;2(10):907-916. doi:10.1038/ni1001-907
48. Xu L-C, Wo Y, Meyerhoff ME, Siedlecki CA. Inhibition of bacterial adhesion and biofilm formation by dual functional textured and nitric oxide releasing surfaces. *Acta Biomater*. 2017;51:53-65. doi:10.1016/j.actbio.2017.01.030
49. Barraud N, Kelso MJ, Rice SA, Kjelleberg S. Nitric oxide : A key mediator of biofilm dispersal with applications in infectious diseases. *Curr Pharm Des*. 2015;21(21):31-42. doi:10.2174/1381612820666140905112822
50. Hossain S, Nisbett L, Boon EM, et al. Discovery of two bacterial nitric oxide-responsive proteins and their roles in bacterial biofilm regulation. *Acc Chem Res*. 2017;50(7):1633-1639. doi:10.1021/acs.accounts.7b00095
51. Arora DP, Hossain S, Xu Y, Boon EM. Nitric oxide regulation of bacterial biofilms. *Methods Mol Biol*. 2014;1085(54):3717-3728. doi:10.1021/bi501476n
52. Schairer DO, Chouake JS, Nosanchuk JD, Friedman AJ. The potential of nitric oxide releasing therapies as antimicrobial agents. *Virulence*. 2012;3(3):271-279. doi:10.4161/viru.20328
53. Ramachandran RA, Lupfer C, Zaki H. The inflammasome: regulation of nitric oxide and antimicrobial host defence. In: *Advances in Microbial Physiology*. Vol 72. Academic Press; 2018:65-115. doi:10.1016/bs.ampbs.2018.01.004
54. Jardeleza C, Foreman A, Baker L, et al. The effects of nitric oxide on *Staphylococcus aureus* biofilm growth and its implications in chronic rhinosinusitis. *Int Forum Allergy Rhinol*. 2011;1(6):438-444. doi:10.1002/alr.20083
55. Schlag S, Nerz C, Birkenstock TA, Altenberend F, Götz F, Go F. Inhibition of staphylococcal biofilm formation by nitrite. *J Bacteriol*. 2007;189(21):7911-7919. doi:10.1128/JB.00598-07
56. Kristian SA, Birkenstock TA, Sauder U, Mack D, Götz F, Landmann R. Biofilm formation induces C3a release and protects *Staphylococcus epidermidis* from IgG and complement deposition and from neutrophil-dependent killing. *J Infect Dis*. 2008;197(7):1028–1035. doi:10.1086/528992
57. Gaupp R, Ledala N, Somerville GA. Staphylococcal response to oxidative stress. *Front Cell Infect Microbiol*. 2012;2(March):33. doi:10.3389/fcimb.2012.00033
58. Carvalho SM, de Jong A, Kloosterman TG, Kuipers OP, Saraiva LM. The *Staphylococcus aureus* α-acetolactate synthase ALS confers resistance to nitrosative stress. *Front Microbiol*. 2017;8(JUL):1-17. doi:10.3389/fmicb.2017.01273
59. Richardson AR, Libby SJ, Fang FC. A Nitric Oxide - Inducible Lactate Dehydrogenase Enables *Staphylococcus aureus* to Resist Innate Immunity. *Science*. 2008;319(March):1672-1676. doi:10.1126/science.1155207
60. Poole RK. Nitric oxide and nitrosative stress tolerance in bacteria. *Biochem Soc Trans*. 2005;33(Pt1):176-180.
61. Flint A, Stintzi A, Saraiva LM. Oxidative and nitrosative stress defences of *Helicobacter* and *Campylobacter* species that counteract mammalian immunity. *FEMS Microbiol Rev*. 2016;40(6):938-960. doi:10.1093/femsre/fuw025
62. Nobre LS, Saraiva LM. Di-iron RICs: Players in Nitrosative-oxidative Stress Defences. In: *Stress and Environmental Regulation of Gene Expression and Adaptation in Bacteria*. Vol 2. Wiley Blackwell; 2016:989-996. doi:10.1002/9781119004813.ch96
63. Cole JA. Anaerobic Bacterial Response to Nitrosative Stress. In: *Advances in Microbial*

Physiology. Vol 72. Academic Press; 2018:193-237. doi:10.1016/bs.ampbs.2018.01.001
64. Spiro S. Nitrous oxide production and consumption: Regulation of gene expression by gas-sensitive transcription factors. *Philos Trans R Soc Lond B Biol Sci*. 2012;367(1593):1213-1225. doi:10.1098/rstb.2011.0309
65. Guillemet E, Leréec A, Tran SL, et al. The bacterial DNA repair protein Mfd confers resistance to the host nitrogen immune response. *Sci Rep*. 2016;6(1):1-12. doi:10.1038/srep29349
66. Richardson AR, Soliven KC, Castor ME, Barnes PD, Libby SJ, Fang FC. The Base Excision Repair System of *Salmonella enterica* serovar Typhimurium Counteracts DNA Damage by Host Nitric Oxide. Stebbins CE, ed. *PLoS Pathog*. 2009;5(5):e1000451. doi:10.1371/journal.ppat.1000451
67. Parrish MC, Chaim IA, Nagel ZD, Tannenbaum SR, Samson LD, Engelward BP. Nitric oxide induced S-nitrosation causes base excision repair imbalance. *DNA Repair (Amst)*. 2018;68:25-33. doi:10.1016/j.dnarep.2018.04.008
68. Nobre LS, Saraiva LM. Effect of combined oxidative and nitrosative stresses on *Staphylococcus aureus* transcriptome. *Appl Microbiol Biotechnol*. 2013;97(6):2563-2573. doi:10.1007/s00253-013-4730-3
69. Stern AM, Zhu J. An Introduction to Nitric Oxide Sensing and Response in Bacteria. In: *Advances in Applied Microbiology*. Vol 87. Academic Press Inc.; 2014:187-220. doi:10.1016/B978-0-12-800261-2.00005-0
70. Richardson AR, Payne EC, Younger N, et al. Multiple targets of nitric oxide in the tricarboxylic acid cycle of *Salmonella enterica* serovar typhimurium. *Cell Host Microbe*. 2011;10(1):33-43. doi:10.1016/j.chom.2011.06.004
71. Tsang LH, Cassat JE, Shaw LN, Beenken KE, Smeltzer MS. Factors contributing to the biofilm-deficient phenotype of *Staphylococcus aureus* sarA mutants. *PLoS One*. 2008;3(10). doi:10.1371/journal.pone.0003361
72. Thomas VC, Sadykov MR, Chaudhari SS, et al. A Central Role for Carbon-Overflow Pathways in the Modulation of Bacterial Cell Death. *PLoS Pathog*. 2014;10(6). doi:10.1371/journal.ppat.1004205
73. Auger C, Lemire J, Cecchini D, Bignucolo A, Appanna VD. The Metabolic Reprogramming Evoked by Nitrosative Stress Triggers the Anaerobic Utilization of Citrate in *Pseudomonas fluorescens*. Cornelis P, ed. *PLoS One*. 2011;6(12):e28469. doi:10.1371/journal.pone.0028469
74. Lindgren JK, Thomas VC, Olson ME, et al. Isolation of Chromosomal and Plasmid DNA from *Staphylococcus epidermidis*. *J Bacteriol*. 2014;196(12):2277-2289. doi:10.1128/JB.00051-14
75. Wu XH, Yu HL, Ba ZY, Chen JY, Sun HG, Han BZ. Sampling methods for NMR-based metabolomics of *Staphylococcus aureus*. *Biotechnol J*. 2010;5(1):75-84. doi:10.1002/biot.200900038
76. Fuchs A, P. Tripet B, Cloud B. Ammons M, Copie V. Optimization of Metabolite Extraction Protocols for the Identification and Profiling of Small Molecule Metabolites from Planktonic and Biofilm *Pseudomonas aeruginosa* Cultures. *Curr Metabolomics*. 2015;4(2):141-147. doi:10.2174/2213235x04666151126203043
77. Ammons MCB, Tripet BP, Carlson RP, et al. Quantitative NMR metabolite profiling of methicillin-resistant and methicillin-susceptible *Staphylococcus aureus* discriminates between biofilm and planktonic phenotypes. *J Proteome Res*. 2014;13(6):2973-2985. doi:10.1021/pr500120c
78. Carvalho SM, Kloosterman TG, Kuipers OP, Neves AR. CcpA Ensures Optimal Metabolic Fitness of *Streptococcus pneumoniae*. *PLoS One*. 2011;6(10). doi:10.1371/journal.pone.0026707
79. Hanke ML, Kielian T. Deciphering mechanisms of staphylococcal biofilm evasion of host immunity. *Front Cell Infect Microbiol*. 2012;2(May):62. doi:10.3389/fcimb.2012.00062
80. Schommer NN, Christner M, Hentschke M, Ruckdeschel K, Aepfelbacher M, Rohde H. *Staphylococcus epidermidis* uses distinct mechanisms of biofilm formation to interfere with phagocytosis and activation of mouse macrophage-like cells 774A.1. *Infect Immun*. 2011;79(6):2267-2276. doi:10.1128/IAI.01142-10
81. Arnaud M, Chastanet A, Débarbouillé M. New Vector for Efficient Allelic Replacement in Naturally Gram-Positive Bacteria. *Appl Environ Microbiol*. 2004;70(11):6887-6891. doi:10.1128/AEM.70.11.6887
82. Decker R, Burdelski C, Zobiak M, et al. An 18 kDa Scaffold Protein Is Critical for *Staphylococcus epidermidis* Biofilm Formation. *PLoS Pathog*. 2015;11(3):1-32.

doi:10.1371/journal.ppat.1004735
83. Rohde H, Burdelski C, Bartscht K, et al. Induction of *Staphylococcus epidermidis* biofilm formation via proteolytic processing of the accumulation-associated protein by staphylococcal and host proteases. *Mol Microbiol*. 2005;55(6):1883-1895. doi:10.1111/j.1365-2958.2005.04515.x
84. Wu T, Jiang Q, Wu D, et al. What is new in lysozyme research and its application in food industry ? A review. *Food Chem*. 2019;274(August 2018):698-709. doi:10.1016/j.foodchem.2018.09.017
85. Wu JA, Kusuma C, Mond JJ, Kokai-Kun JF. Lysostaphin Disrupts *Staphylococcus aureus* and *Staphylococcus epidermidis* Biofilms on Artificial Surfaces. *Antimicrob Agents Chemother*. 2003;47(11):3407-3414. doi:10.1128/AAC.47.11.3407-3414.2003
86. Schaeffer CR, Hoang T-MN, Sudbeck CM, et al. Versatility of Biofilm Matrix Molecules in *Staphylococcus epidermidis* Clinical Isolates and Importance of Polysaccharide Intercellular Adhesin Expression during High Shear Stress. *mSphere*. 2016;1(5). doi:10.1128/msphere.00165-16
87. Lindgren JK. *Isolation of Chromosomal and Plasmid DNA from Staphylococcus Epidermidis*. Vol 1106. (Fey PD, ed.). Humana Press; 2014. doi:10.1007/978-1-62703-736-5_17
88. Kocianova S, Vuong C, Yao Y, et al. Key role of poly-γ-dl-glutamic acid in immune evasion and virulence of *Staphylococcus epidermidis*. *J Clin Invest*. 2005;115(3):688-694. doi:10.1172/jci23523
89. Li X, Bosch-Tijhof CJ, Wei X, et al. Efficiency of chemical versus mechanical disruption methods of DNA extraction for the identification of oral Gram-positive and Gram-negative bacteria. *J Int Med Res*. 2020;48(5):1-12. doi:10.1177/0300060520925594
90. Rantakokko-Jalava K, Jalava J. Optimal DNA isolation method for detection of bacteria in clinical specimens by broad-range PCR. *J Clin Microbiol*. 2002;40(11):4211-4217. doi:10.1128/JCM.40.11.4211-4217.2002
91. Boer R, Peters R, Gierveld S, Scurman T, Kooistra-Smid M, Savelkoul P. Improved detection of microbial DNA after bead-beating before DNA isolation. *J Microbiol Methods*. 2010;80(2):209-211. doi:10.1016/j.mimet.2009.11.009
92. Bruin OM, Birnboim HC. A method for assessing efficiency of bacterial cell disruption and DNA release. *BMC Microbiol*. 2016;16(1):197. doi:10.1186/s12866-016-0815-3
93. Larson TR, Yother J. *Streptococcus pneumoniae* capsular polysaccharide is linked to peptidoglycan via a direct glycosidic bond to β-D-N-acetylglucosamine. *Proc Natl Acad Sci U S A*. 2017;114(22):5695-5700. doi:10.1073/pnas.1620431114
94. Terrasse R, Amoroso A, Vernet T, Di Guilmi AM. *Streptococcus pneumoniae* GAPDH Is Released by Cell Lysis and Interacts with Peptidoglycan. *PLoS One*. 2015;10(4):e0125377. doi:10.1371/journal.pone.0125377
95. Islam MS, Aryasomayajula A, Selvaganapathy PR. A Review on Macroscale and Microscale Cell Lysis Methods. *Micromachines*. 2017;8(3). doi:10.3390/mi8030083
96. Mack D, Rohde H, Dobinsky S, et al. Identification of three essential regulatory gene loci governing expression of *Staphylococcus epidermidis* polysaccharide intercellular adhesin and biofilm formation. *Infect Immun*. 2000;68(7):3799-3807. doi:10.1128/IAI.68.7.3799-3807.2000
97. Buckner MMC, Ciusa ML, Piddock LJ V. Strategies to combat antimicrobial resistance : anti-plasmid and plasmid curing. *FEMS Microbiol Rev*. 2018;42(6):781-804. doi:10.1093/femsre/fuy031
98. Kwong SM, Ramsay JP, Jensen SO, Firth N. Replication of Staphylococcal Resistance Plasmids. *Front Microbiol*. 2017;8(November):1-16. doi:10.3389/fmicb.2017.02279
99. Schumacher MA. Bacterial plasmid partition machinery : a minimalist approach to survival. *Curr Opin Struct Biol*. 2012;22(1):72-79. doi:10.1016/j.sbi.2011.11.001
100. Brendler T, Reaves L, Austin S. Interplay between Plasmid Partition and Postsegregational Killing Systems. *J Bacteriol*. 2004;186(8):2504-2507. doi:10.1128/JB.186.8.2504
101. Zipperer A, Konnerth MC, Laux C, et al. Human commensals producing a novel antibiotic impair pathogen colonization. *Nature*. 2016;535(7613):511-516. doi:10.1038/nature18634
102. Winstel V, Kühner P, Krismer B, Peschel A, Rohde H. Transfer of plasmid DNA to clinical coagulase-negative staphylococcal pathogens by using a unique bacteriophage. *Appl Environ Microbiol*. 2015;81(7):2481-2488. doi:10.1128/AEM.04190-14
103. Geiger T, Francois P, Liebeke M, et al. The Stringent Response of *Staphylococcus aureus* and Its Impact on Survival after Phagocytosis through the Induction of Intracellular PSMs

Expression. 2012;8(11). doi:10.1371/journal.ppat.1003016
104. Monk IR, Shah IM, Xu M. Transforming the Untransformable: Application of Direct Transformation To Manipulate Genetically *Staphylococcus aureus* and *Staphylococcus epidermidis*. *MBio*. 2012;3(2):e00277-11. doi:10.1128/mBio.00277-11.Editor
105. Kodumal SJ, Santi D V. DNA ligation by selection. *Biotechniques*. 2004;37(1):34-40. doi:10.2144/04371bm02
106. Matsumura I. Why Johnny can't clone: Common pitfalls and not so common solutions. *Biotechniques*. 2015;59(3):4-13. doi:10.2144/000114324
107. Jajesniak P, Wong TS. QuickStep-Cloning: a sequence-independent, ligation-free method for rapid construction of recombinant plasmids. *J Biol Eng*. 2015;9(15). doi:10.1186/s13036-015-0010-3
108. Freitas C. *How Staphylococcus epidermidis and Staphylococcus aureus cope with oxidative and nitrosative stress*. [master's theis]. Oeiras: Instituto de Tecnologia Química e Biológica António Xavier;2018.
109. Méric G, Mageiros L, Pensar J, et al. Disease-associated genotypes of the commensal skin bacterium *Staphylococcus epidermidis*. *Nat Commun*. 2018;9(1):1-11. doi:10.1038/s41467-018-07368-7
110. Yao T, Asayama Y. Animal-cell culture media: History, characteristics, and current issues. *Reprod Med Biol*. 2017;16(2):99-117. doi:10.1002/rmb2.12024
111. Kawakami T, Kawamura K, Fujimori K, Koike A, Amano F. Influence of the culture medium on the production of nitric oxide and expression of inducible nitric oxide synthase by activated macrophages in vitro. *Biochem Biophys Reports*. 2016;5:328-334. doi:10.1016/j.bbrep.2016.01.006
112. Missiakas DM, Schneewind O. Growth and laboratory maintenance of *Staphylococcus aureus*. *Curr Protoc Microbiol*. 2013;CHAPTER 9:Unit. 9C.1 doi:10.1002/9780471729259.mc09c01s28
113. Boles BR, Horswill AR. Staphylococcal biofilm disassembly. *Trends Microbiol*. 2011;19(9):449-455. doi:10.1016/j.tim.2011.06.004
114. Cue D, Lei MG, Lee CY. Genetic regulation of the intercellular adhesion locus in staphylococci. *Front Cell Infect Microbiol*. 2012;2:38. doi:10.3389/fcimb.2012.00038
115. Freitas AI, Lopes N, Oliveira F, Br S. Comparative analysis between biofilm formation and gene expression in *Staphylococcus epidermidis isolates*. *Future Microbiol*. 2018;13(4):415-427.
116. Gaio V, Cerca N. Biofilm released cells can easily be obtained in a fed-batch system using ica + but not with ica- isolates. *PeerJ*. 2020;8:e9549. doi:10.7717/peerj.9549
117. Wo Y, Xu LC, Li Z, Matzger AJ, Meyerhoff ME, Siedlecki CA. Antimicrobial nitric oxide releasing surfaces based on: S-nitroso-N-acetylpenicillamine impregnated polymers combined with submicron-textured surface topography. *Biomater Sci*. 2017;5(7):1265-1278. doi:10.1039/c7bm00108h
118. DeFrancesco AS, Masloboeva N, Syed AK, et al. Genome-wide screen for genes involved in eDNA release during biofilm formation by *Staphylococcus aureus*. *Proc Natl Acad Sci U S A*. 2017;114(29):E5969-E5978. doi:10.1073/pnas.1704544114
119. Knobloch JK-M, Nedelmann M, Kiel K, et al. Establishment of an Arbitrary PCR for Rapid Identification of Tn917 Insertion Sites in *Staphylococcus epidermidis*: Characterization of Biofilm-Negative and Nonmucoid Mutants. *Microbiology*. 2003;69(10):5812-5818. doi:10.1128/AEM.69.10.5812
120. Hyduke DR, Jarboe LR, Tran LM, Chou KJY, Liao JC. Integrated network analysis identifies nitric oxide response networks and dihydroxyacid dehydratase as a crucial target in *Escherichia coli*. *Proc Natl Acad Sci U S A*. 2007;104(20):8484-8489. doi:10.1073/pnas.0610888104
121. Otto M. *Staphylococcus epidermidis* pathogenesis. *Methods Mol Biol*. 2014;1106:17-31. doi:10.1007/978-1-62703-736-5_2
122. França A, Pérez-cabezas B, Correia A, Pier GB, Cerca N, Vilanova M. Biofilm-Released Cells Induce a Prompt and More Marked In vivo Inflammatory-Type Response than Planktonic or Biofilm Cells. *Front Microbiol*. 2016;7(September):1-12. doi:10.3389/fmicb.2016.01530
123. Gaio V, Cerca N. Cells released from *S . epidermidis* biofilms present increased antibiotic tolerance to multiple antibiotics. *PeerJ.* 2019;*7:e6884*. doi:10.7717/peerj.6884
124. Schoenfelder SMK, Lange C, Prakash SA, et al. The small non-coding RNA rsae influences extracellular matrix composition in *Staphylococcus epidermidis* biofilm communities. *PLoS Pathog*. 2019;15(3):1-31. doi:10.1371/journal.ppat.1007618

125. Wijesinghe G, Dilhari A, Gayani B, Kottegoda N, Samaranayake L, Weerasekera M. Influence of Laboratory Culture Media on in vitro Growth, Adhesion, and Biofilm Formation of *Pseudomonas aeruginosa* and *Staphylococcus aureus*. *Med Princ Pract*. 2019;28(1):28-35. doi:10.1159/000494757
126. Stepanović S, Vuković D, Hola V, et al. Quantification of biofilm in microtiter plates: Overview of testing conditions and practical recommendations for assessment of biofilm production by staphylococci. *APMIS*. 2007;115(8):891-899. doi:10.1111/j.1600-0463.2007.apm_630.x
127. Ali H, Greco-Stewart VS, Jacobs MR, et al. Characterization of the growth dynamics and biofilm formation of *Staphylococcus epidermidis* strains isolated from contaminated platelet units. *J Med Microbiol*. 2014;63(PART 6):884-891. doi:10.1099/jmm.0.071449-0
128. Chen X, Thomsen TR, Winkler H, Xu Y. Influence of biofilm growth age, media, antibiotic concentration and exposure time on *Staphylococcus aureus* and *Pseudomonas aeruginosa* biofilm removal in vitro. *BMC Microbiol*. 2020;20(1):264. doi:10.1186/s12866-020-01947-9
129. Fuchs S, Pané-Farré J, Kohler C, Hecker M, Engelmann S. Anaerobic gene expression in *Staphylococcus aureus*. *J Bacteriol*. 2007;189(11):4275-4289. doi:10.1128/JB.00081-07
130. Otto M. Staphylococcal biofilms. *Curr Top Microbiol Immunol*. 2008;322:207-228. doi:10.1007/978-3-540-75418-3_10
131. Pedroza-Davila U, Uribe-Alvarez C, Morales-Garcia L, et al. Metabolism, ATP production and biofilm generation by *Staphylococcus epidermidis* in either respiratory or fermentative conditions. January 2020. doi:10.21203/rs.2.22319/v1
132. Yeswanth S, Nanda Kumar Y, Venkateswara Prasad U, Swarupa V, Koteswara rao V, Venkata Gurunadha Krishna Sarma P. Cloning and characterization of l-lactate dehydrogenase gene of *Staphylococcus aureus*. *Anaerobe*. 2013;24:43-48. doi:10.1016/j.anaerobe.2013.09.003
133. Somerville GA, Saïd-Salim B, Wickman JM, Raffel SJ, Kreiswirth BN, Musser JM. Correlation of acetate catabolism and growth yield in *Staphylococcus aureus*: Implications for host-pathogen interactions. *Infect Immun*. 2003;71(8):4724-4732. doi:10.1128/IAI.71.8.4724-4732.2003
134. Onyango LA, Alreshidi MM. Adaptive Metabolism in Staphylococci: Survival and Persistence in Environmental and Clinical Settings. *J Pathog*. 2018;2018(1092632):1-11. doi:10.1155/2018/1092632
135. Shapiro JA, Nguyen VL, Chamberlain NR. Evidence for persisters in *Staphylococcus epidermidis* RP62a planktonic cultures and biofilms. *J Med Microbiol*. 2011;60(7):950-960. doi:10.1099/jmm.0.026013-0
136. Vitko NP, Spahich NA, Richardson AR. Glycolytic dependency of high-level nitric oxide resistance and virulence in *Staphylococcus aureus*. *MBio*. 2015;6(2). doi:10.1128/mBio.00045-15
137. Wu YY, Wu YY, Zhu T, et al. *Staphylococcus epidermidis* SrrAB regulates bacterial growth and biofilm formation differently under oxic and microaerobic conditions. *J Bacteriol*. 2015;197(3):459-476. doi:10.1128/JB.02231-14
138. Duportet X, Aggio RBM, Carneiro S, Villas-Bôas SG. The biological interpretation of metabolomic data can be misled by the extraction method used. *Metabolomics*. 2012;8(3):410-421. doi:10.1007/s11306-011-0324-1
139. Liebeke M, Dörries K, Meyer H, Lalk M. Metabolome Analysis of Gram-Positive Bacteria such as *Staphylococcus aureus* by GC-MS and LC-MS. *Methods Mol Biol*. 2012;815:377-398. doi:10.1007/978-1-61779-424-7_28
140. Ser Z, Liu X, Tang NN, Locasale JW. Extraction parameters for metabolomics from cell extracts. *Anal Biochem*. 2015;475:22-28. doi:10.1016/j.coviro.2015.09.001.Human
141. Sapcariu SC, Kanashova T, Weindl D, Ghelfi J, Dittmar G, Hiller K. Simultaneous extraction of proteins and metabolites from cells in culture. *MethodsX*. 2014;1(1):74-80. doi:10.1016/j.mex.2014.07.002
142. Stipetic LH. *Metabolomics as a tool to explore the staphylococcal biofilm* [PhD thesis]. Glasgow: University of Glasgow*;* 2016.
143. Zhang Q, Zheng X, Wang Y, et al. Comprehensive optimization of the metabolomic methodology for metabolite profiling of *Corynebacterium glutamicum. Appl Microbiol Biotechnol*. 2018;102(16):7113-7121. doi:10.1007/s00253-018-9095-1
144. Bolten CJ, Kiefer P, Letisse F, Portais JC, Wittmann C. Sampling for metabolome analysis of microorganisms. *Anal Chem*. 2007;79(10):3843-3849. doi:10.1021/ac0623888
145. Ramos A, Boels IC, De Vos WM, Santos H. Relationship between glycolysis and

exopolysaccharide biosynthesis in *Lactococcus lactis*. *Appl Environ Microbiol*. 2001;67(1):33-41. doi:10.1128/AEM.67.1.33-41.2001
146. Paixão L, Oliveira J, Veríssimo A, et al. Host glycan sugar-specific pathways in *Streptococcus pneumonia*: Galactose as a key sugar in colonisation and infection. *PLoS One*. 2015;10(3). doi:10.1371/journal.pone.0121042
147. Ramos A, Neves AR, Santos H. Metabolism of lactic acid bacteria studied by nuclear magnetic resonance. In: *Lactic Acid Bacteria: Genetics, Metabolism and Applications*. Springer Netherlands; 2002:249-261. doi:10.1007/978-94-017-2029-8_15
148. Neves AR, Pool WA, Kok J, Kuipers OP, Santos H. Overview on sugar metabolism and its control in *Lactococcus lactis* - The input from in vivo NMR . *FEMS Microbiol Rev*. 2005;29(3):531-554. doi:10.1016/j.fmrre.2005.04.005
149. Sana T, Fischer S. Maximizing Metabolite Extraction for Comprehensive Metabolomics Studies of Erythrocytes. 2007:8. www.agilent.com/chem/metabolomics. Accessed June 8, 2020.
150. Geiger T, Francois P, Liebeke M, Fraunholz M, Goerke C. The stringent response of *Staphylococcus aureus* and its impact on survival after phagocytosis through the induction of intracellular PSMs expression. 8(11). doi:10.1371/journal.ppat.1003016
151. Bae T, Schneewind O. Allelic replacement in *Staphylococcus aureus* with inducible counter-selection. 2006;55:58-63. doi:10.1016/j.plasmid.2005.05.005
152. Prax M, Lee CY, Bertram R, Bertram R. An update on the molecular genetics toolbox for staphylococci. *Microbiology*. 2013;159(Pt_3):421-435. doi:10.1099/mic.0.061705-0

7 Appendices

7.1 Primers and mutant construction

Table 7.1 - List of primers used in this study and in the construction of the pMAD_*hmp* plasmid

	Primer	Sequence (5' →3')	Enzyme
pBASE6-*hmp*	*hmp* _fw_A	GGTGATATCGCTTCCATGTTCCACATGCT	EcoRV
	hmp _rev_A	CGTCCCGGGTCCATACGCTTTTGCCCACG	XmaI
	*hmp*_fw_B	TGACCCGGGCTGGCGTAGGTATGACACCA	XmaI
	*hmp*_rev_B	TTTGAATTCCACAGTCACCAACTCCTTGC	EcoRI
pBASE6-erm/lox1 or 2-*hmp*	2*hmp* _fw_A	GGTGTCGACGCTTCCATGTTCCACATGCT	SalI
	2*hmp* _rev_A	CGTGCTAGCTCCATACGCTTTTGCCCACG	NheI
	2*hmp*_fw_B	TTAGAGCTCCTGGCGTAGGTATGACAC	SacI
	2*hmp*_rev_B	TTTGAATTCCACAGTCACCAACTCCTTGC	EcoRI
	Erm_fw	GCTAGCCCTACCGTTCGTAT	-
	Erm_rev	GAGCTCGGTACCCTACCGTT	-
	A_Erm	**ATACGAACGGTAGGGCTAGC**TCCATACGCTTTTGCCCACG	-
	Erm_B	**AACGGTAGGGTACCGAGCTC**CTGGCGTAGGTATGACAC	-
Colony PCR	pMAD_fw	GCAACGCGGGCATCCCGATG	-
	pMAD_rev	CCCAATATAATCATTTATCAACTCTTTTACACTTAAATTTCC	-
	pBASE6_fw	CAATCCGTTCTGCAGGCATG	-
	pBASE6_rev	ACTCATCGCAGTGCAGC	-
pMAD-*hmp*	pMAD_*hmp*_A	TTCGTGGATCCTAATTAAATCTTCTAATATG	BamHI
	pMAD_*hmp*_B	**CCTCACTATTTTGATTAG**TAGCTATTATCCTATATTTC	-
	pMAD_*hmp*_C	**GCGTTTATTTCGTTTAGT**TTAAAGAATTAAATTATG	-
	pMAD_*hmp*_D	ATTATGTCGACTGACAGTCATACTATACC	SalI

Underlined: Enzyme restriction site
Bold: Overlapping/complementary sequence

7.1.1 pMAD-*hmp* plasmid

The pMAD plasmid was constructed by Aurnaud, M. and coworkers to allow allelic replacement in nontransformable low GC, Gram-positive bacteria[81]. This plasmid has an Erm resistance gene, is temperature sensitive and contains the *bgaB* gene, which allows for the colorimetric white/blue screening of correctly transformed bacteria using X-Gal[81]. Previously, in our laboratory, pMAD was used for the construction of the pMAD-*hmp* plasmid (Fig. 7.1) as follows. The upstream (663 bp) and downstream (828 bp) regions of the *hmp* gene (1145 bp) were PCR amplified from *S. epidermidis* 1457 chromosomal DNA by using the primer pairs pMAD_*hmp*_A / pMAD_*hmp*_B and pMAD_*hmp*_C / pMAD_*hmp*_D (Table 7.1), respectively. The resulting PCR products were fused to a spectinomycin cassette by overlap extension PCR (SOE-PCR)[108], using the outward primers pMAD_*hmp*_A and pMAD_*hmp*_D. The PCR product (2487 bp) obtained, and pMAD were digested with BamHI and SalI and ligated as described in Table 7.2. The resulting pMAD-*hmp* plasmid (Table 2.1) was then transformed into *E. coli* DH5α and the insert region of pMAD-*hmp* plasmid was confirmed by sequencing (STAB VIDA). After confirmation, pMAD-*hmp* was sequentially transformed into *S. aureus* RN4220 and *S. epidermidis* 1457-M12, always grown at a permissive temperature (30ºC). To confirm the presence of the plasmid inside cells, the resulting colonies were screened by colony PCR using the primer pair pMAD_fw / pMAD_rev (Table 7.1, and 7.4). The full protocol for the construction of

mutants by allelic replacement mutagenesis using pMAD is described by Aurnaud, M. et al[81]. Here, we make a description of the steps that follow mutant construction from the point where we left it. Briefly, the pMAD plasmid containing the spectinomycin resistance cassette flanked by regions of the gene to be replaced is transformed into the strain of interest. Transformed staphylococci are then plated on TSA containing spectinomycin and/or erythromycin and X-Gal and grown at 30ºC, the permissive temperature for replication of the plasmid inside cells. Transformed isolated blue colonies are picked up and grown in TSB at 42ºC in the absence of antibiotic. Cultures are then plated on TSA containing X-Gal and antibiotic(s) and incubated at 42ºC. At this temperature, the plasmid is not able to replicate and is under selective pressure due to the presence of antibiotic, which prompts plasmid integration into the bacterial genome. The presence of white colonies indicates candidates where double cross over events and loss of vector have occurred.

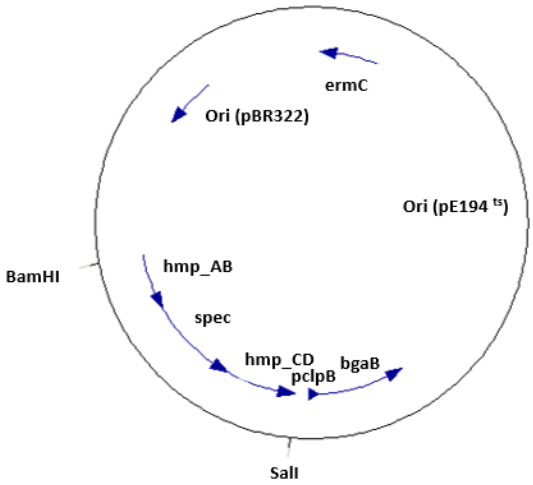

Figure 7.1 - pMAD-*hmp* plasmid. The fragment *hmp*_AB_spec_*hmp*_CD was previously constructed by SOE-PCR and ligated into pMAD plasmid. Spec, spectinomycin resistance gene; Original sequences of pMAD plasmid: Ori(pBR322) and Ori (pE194^{ts}), derived from plasmids pBR322 and pE194^{ts}, respectively; *ermC*, an erythromycin resistance gene, and bgaB, coding for β-galactosidase, under the control of the staphylococci promotor - pclpB.

7.1.2 pBASE-*hmp* plasmid

pBASE6[103] is a temperature sensitive shuttle plasmid that allows for counter selection with the antisense *secY* RNA. pBASE6-erm/lox1[101] and pBASE6-erm/lox2[102] plasmids were derived from pBASE6 by addition of an erythromycin resistance cassette, and differ only in a few amino acids. These vectors were used in the construction of the pBASE6-*hmp*, pBASE6-erm/lox1-*hmp* and pBASE6-erm/lox2-*hmp* plasmids (Fig. 2.1, 2.2, 2.3 and 7.2). Full protocols for the construction of mutants by allelic replacement mutagenesis using pBASE6 and pBASE6-erm/lox1 and 2 plasmids are shown in Geiger,T 2012, Zipperer, A. 2016 and Winste, V. 2015[101,102,150]. A description of the steps that follow mutant construction from the point where we left it (chapter 2) is presented here. In brief, the pBASE6 and pBASE6-erm/lox1 or 2 plasmids, containing the upstream and downstream fragments of the gene to be deleted, are transformed into *Staphylococcus* in the absence and presence of erythromycin, respectively, at 30ºC. Transformed colonies are then grown at 43ºC, a nonpermissive temperature for plasmid replication, in the presence of anhydrotetracycline[151]. The anhydrotetracycline activates the plasmid's *Pxyl/tetO* promoter, formed from insertion of the *tet*

operator into the P_{xylA} promotor from *Bacillus subtilis*[152], allowing for the transcription of the antisense *secY* RNA. Once expressed, the antisense *secY* RNA hampers the expression of the bacterial chromosomal *secY* gene that codes a membrane protein essential for bacterial growth and survival. In this way, bacteria that only contain the desired sequence inserted into the genome will survive and those that have integrated the entire plasmid will not[151,152].

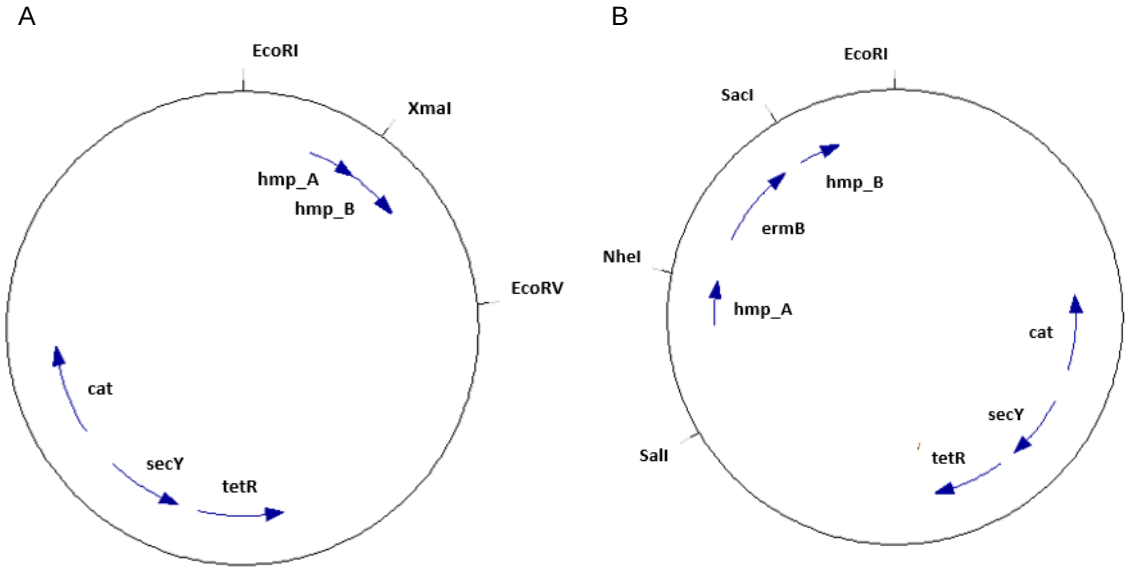

Figure 7.2 - A) pBASE6_*hmp* plasmid. The fragment *hmp*_A-*hmp*_B, lacking an internal region of the *hmp* gene, was ligated into the pBASE6 plasmid, which contains cat, a chloramphenicol acetyltransferase repressor of TetR, a tetracycline resistance element and an antisense RNA – secY, under the control of the Pxyl/tetO promotor[152] (not shown) B) pBASE6-erm/lox1_*hmp* and pBASE6-erm/lox2_*hmp* plasmids. These two plasmids differ in only six amino acids in positions 1281 to 1283 and 1286 to 1288. They have the same genetic elements as the pBASE6_*hmp* plasmid plus an erythromycin resistance cassette between the *hmp*_A and the *hmp*_B sequences.

7.2 Molecular biology Methods

7.2.1 *S. epidermidis* 1457-M12 electroporation

To transform the pMAD-*hmp* plasmid into *S. epidermidis* 1457-M12, 8.4 µg of plasmid DNA was added to competent cells of 1457-M12 thawed at RT for 5 min. The cells were transferred to a 1 mm electroporation cuvette (Bio-Rad), incubated at room temperature for 30 min, and then electroporated at 2 Kv for 2.5 ms (MicroPulser Electroporator, Bio-Rad). Immediately after the pulse, 950 µL of SMMP media (equal parts of 2X SMM buffer – sucrose 1 M, maleic acid 0.04 M and magnesium chloride hexahydrate 0.04 M – and 4X Penassay broth – beef extract 6 g/L, yeast extract 6 g/L, peptone 20 g/L, glucose 4 g/L, sodium chloride 17.5 g/L, dipotassium phosphate 14.72 g/L and monopotassium phosphate 5.28 g/L) was added to the electroporated cells, which were then placed at 30ºC and 200 rpm for 4 h. After incubation, cells were centrifuged at 5000 x *g* for 5 min (RT), 900 µL of the supernatant was discarded and the pellet was resuspended in the remaining supernatant (*circa* 100 µL). The 100 µL cells were divided (2 x 50 µL), plated in TSA supplemented with erythromycin (5 µg/mL Sigma) and spectinomycin (100 µg/mL, Sigma) and incubated o/n at 30ºC.

7.2.2 *S. epidermidis* 1457 genomic DNA extraction

Extraction of genomic DNA from *S. epidermidis* 1457-M12 was made using the NZY Tissue gDNA Isolation kit (NZY). The cell pellet of 1 mL of overnight culture centrifuged at 6800 x *g* for 5 min was resuspended in 25 µL of 50 mM Tris-HCl, pH 8 (Carl-Roth, CARLO ERBA), and then digested with lysostaphin (0.08 mg/mL, Sigma-Aldrich), lysozyme (4 mg/mL, Sigma-Aldrich) and mutanolysin (0.08 KU/mL, Sigma-Aldrich), in a 37ºC water bath for 1 h. Buffer NT1 was added and the protocol was finished according to kits instructions.

7.2.3 Fragment amplification, enzyme restriction and ligation reactions

For the construction of the pBASE6-*hmp*, pBASE6-erm/lox1-*hmp* and pBASE6-erm/lox2-*hmp* plasmids, the PCR reaction mixtures to amplify regions of the genome and plasmid fragments are shown in Table 7.2 and the reactions for enzymatic digestions and ligations of fragments and plasmids are shown in Table 7.3. The products of the enzymatic digestions were purified with the QIAquick® PCR Purification kit (Qiagen) and quantified in a Nanodrop ND-1000 UV-visible spectrophotometer (Thermo Fisher Scientific).

Table 7.2 - Reaction mix (V_{total}= 50 µL) of the performed PCRs for fragment amplification

Component	**Amount (µL)**
10µM Primer forward	2.5 µL
10µM Primer reverse	2.5 µL
Template DNA	1 µL
10 mM dNTPs	1 µL
Phusion DNA polymerase (NEB)	0.5 µL
5x Phusion HF buffer (NEB)	10 µL
Milli-Q water	32.5 µL

Table 7.3 - Reagents and conditions used in fragments and plasmid restriction digestion and ligation reactions

Component	**Amount**	**Total reaction volume and incubation conditions**
Digestion		50 µL 37ºC, 2 h
DNA (insert or plasmid)	1.1 µg	
10X NEBuffer	5 µL	
Restriction endonuclease 1	3.5 µL	
Restriction endonuclease 2	3.5 µL	
Milli-Q water	to 50 µL	
Ligation		20 µL 16ºC, 16 h
T4 DNA ligase	1 µL	
10X T4 DNA ligase buffer	2 µL	
Plasmid DNA	50 ng	
Insert DNA	20x moles of plasmid	

7.2.4 E. coli DC10B strain transformation

A 1% (v/v) pre-inoculum of DC10B cells in LB media (Difco) was grown until an OD_{600} of about 0.5. Then, 1300 µL of culture were collected and centrifuged at 1677 x *g* for 5 min at RT. The pellet was resuspended in 750 µL of ice-cold $CaCl_2$ (100 mM, Merck), incubated on ice for 1 h and the pBASE6_*hmp*, pBASE6-erm/lox1_*hmp* and pBASE6-erm/lox2_*hmp* plasmids were added to a final concentration of 100 ng/µL. The tubes were left on ice for 30 min, followed by a heat shock at 42ºC for 45 sec, and recovery on ice for 2 min. Then, the samples were incubated for 1 h at 37ºC and 150 rpm with 900 µL of LB media (Difco) and centrifuged at 1677 x *g*, for 5 min, at RT. The pellet was resuspended in 100 µL of the supernatant, plated in LA media (Difco), which was supplemented with erythromycin, for the growth of the strains transformed with pBASE6-erm/lox1_*hmp* or pBASE6-erm/lox2_*hmp*, and grown at 30ºC.

7.2.5 Colony PCR

To screen for positive clones, *S. epidermidis* 1457-M12 and *E. coli* DC10B individual colonies were picked up from TSA (Difco) and LA media (Difco), respectively. Two different colony PCR methods were tested. First, each picked colony was scratched in a PCR tube and microwaved at 80 w for 10 min. Then, the reaction mixtures (Table 7.4), were added into the tubes where the colonies were scratched. Secondly, each picked colony was resuspended in 50 µL of sterile milli-Q water and placed in boiling water for 5 min, followed by a spin down. In this technique, 15 µL of the supernatant was used for a PCR reaction using the primer mix described in Table 7.4.

Table 7.4 - Reaction mix of the performed colony PCRs

Component	Amount	Total reaction volume
10 µM pMAD_fw or pBASE6_fw	1.5 µL	30 µL
10 µM pMAD_rev or PBASE6_rev	1.5 µL	
10 mM dNTPs	0.6 µL	
Taq DNA polymerase (NEB)	0.18 µL	
10x ThermoPol buffer (NEB)	3 µL	
Milli-Q water or Milli-Q water + supernatant	23.22 µL	